Fast Valuation of Options under Parameter Uncertainty

Hanna Wu
Lund University

ABSTRACT

Option valuation is typically done under the unrealistic assumption of perfect knowledge about model parameters. This thesis shows that risk-neutral valuation, while still adressing the parameter uncertainty, can be computed for a variety of models within the Fourier framework. This results in a computationally inexpensive method for valuating options. A study of S&P500 index option data shows that the method improves the predictive performances of the Black&Scholes, Merton and Heston models.

Keywords: Option valuation, parameter uncertainty, Fourier methods, risk neutral valuation formula.

CONTENTS

ABSTRACT **i**

CONTENTS **ii**

ACKNOWLEDGMENTS **iv**

NOTATION AND ACRONYMS **v**

1 INTRODUCTION **1**
1.1 Overview of the thesis 1

2 THEORETICAL BACKGROUND **3**
2.1 Probability theory 3
2.2 Basics in financial modeling 4
2.3 Valuation theory 5
2.4 The concept of parameter uncertainty 6
2.5 Valuation using Fourier methods 7

3 FAST VALUATION UNDER PARAMETER UNCERTAINTY **10**
3.1 Fourier methods under parameter uncertainty 10
3.2 Application on stock price models 12
3.2.1 The Black&Scholes model 12
3.2.2 The Merton model 13
3.2.3 The Heston model 15
3.2.4 The Bates model 16

4 SIMULATION STUDY **17**
4.1 Implementation of the Fourier method 18
4.2 Black&Scholes 18
4.3 Merton 19
4.4 Heston 23
4.5 Bates 26

5 EMPIRICAL STUDY **29**
5.1 Least Squares method 29
5.1.1 Results 30
5.2 Unscented Kalman Filter 43
5.2.1 Results 44

6 CONCLUSIONS **57**
6.1 Further work 57

A TRIANGULAR DISTRIBUTION IN THE B&S MODEL **58**

BIBLIOGRAPHY **60**

ACKNOWLEDGMENTS

I would like to thank my supervisor Erik Lindström, associate professor at Lund University, for introducing me to the interesting subject of parameter uncertainty. He has given me great support throughout my work and I am truly glad to have been given the opportunity to work with him.

I am also grateful to Aron Wennman, PhD student at KTH Royal Institute of Technology, for helping me with some of the theoretical background and to Magnus Wiktorsson, associate professor at Lund University, for examining this thesis.

Finally, I would like to acknowledge Ted and Johan for being great role-models and thank my friends Aron, Danial, Emma, Fredrik, Linn, Palle, Teo, Tobias, Viktor and many more for making my last semester as a student more than enjoyable.

NOTATION AND ACRONYMS

$\lvert\cdot\rvert$	the Euclidean norm
Ω	sample space
$\mathcal{F}$	collection of events
φ	characteristic function
$\Re[\cdot]$	the real part
$\mathbb{I}(\cdot)$	the indicator function
$\mathbb{E}(\cdot)$	the expectation
$\mathbb{V}(\cdot)$	the variance
$F_X(x), F(x)$	distribution function of X
$X \sim F, X \in F$	X has distribution (function) F
$X := Y$	X denotes Y

B&S	Black & Scholes
i.i.d.	independent and identically distributed
LS	least squares
PDF	probability density function
RMSE	root mean square error
RNVF	risk-neutral valuation formula
SDE	stochastic differential equation
UKF	unscented Kalman filter

Chapter 1

INTRODUCTION

Options are financial contracts which are common tools for risk reduction and speculation. However, valuation of options is typically done under the assumption of perfect knowledge. For example, the widely used Risk Neutral Valuation formula (RNVF) for pricing financial contracts assumes that the history of the underlying asset is perfectly known, something that is rather unlikely. When market participants value options they usually fit a model to empirical data which requires estimation of the model parameters. Different investors will obtain different parameters estimate depending on the data, from which we can argue for the existence of parameter uncertainty in the market, something that the RNVF does not take into account.
The theory behind valuation under the risk-neutral measure, while still addressing the parameter uncertainty in statistical models, was discussed in [11] and [12]. Adding parameter uncertainty into the framework of known models, resulted in new models which we *modified* or *corrected* models in this thesis. In the former paper, the modified Black&Scholes and Merton models were found to out-perform their non-corrected counterparts. The main weakness however was the computational aspects, as Monte Carlo methods were used in the paper.
The purpose of this thesis is to derive the parameter corrections within the Fourier framework, since Fourier methods are computationally fast, accurate and applicable to a wide range of models. We show that this can be readily done for models where the characteristic function is on an exponentially affine form. A simulation study and an empirical study are then made, where we price options in the modified Black&Scholes, Merton, Heston and Bates models in comparison with their standard counterparts.

1.1 Overview of the thesis

Chapter 2 is a collection of the theoretical background used in this thesis. We state some relevant results from probability theory and introduce the basics of financial modeling and valuation theory. We then describe the concept of parameter uncertainty in detail and derive how options are valued using Fourier methods.
Chapter 3 describes the method developed in this thesis. We show that risk-neutral valuation under parameter uncertainty can be applied with the Fourier method, re-

stricted for models having well-defined and exponentially affine characteristic functions. The derived technique is then applied to four common stock price models in contemporary literature, namely the Black&Scholes, Merton, Heston and Bates models.
Chapter 4 is a simulation study where we price European call options for different strikes and maturities. The implied volatility is then computed. The results show that the corrected models will generate a volatility smile which is consistent with empirical observations.
Chapter 5 is an empirical study where S&P 500 option values has been collected. The weighted least-squares with penalty and the unscented Kalman filter are used to estimate model parameters in sample and to predict out of sample. The Root Mean Square Error (RMSE) is computed in order to compare model performances. The thesis is concluded in Chapter 6.

Chapter 2

THEORETICAL BACKGROUND

2.1 Probability theory

The characteristic function is an important ingredient in the Fourier method. We therefore define it and state some useful theorems. In addition, we state a result known as the Fubini-Tonelli theorem which will be used in the proof of Proposition 1 in Chapter 3. A more detailed treatment on probability and measure theory can be found in e.g. [8] and [14].

Definition 1. (Characteristic function) *The characteristic function of a random variable X is a function $\varphi_X : \mathbb{R} \to \mathbb{C}$ such that*

$$\varphi_X(u) \;=\; \mathbb{E}(e^{iuX}) = \int_{\mathbb{R}} e^{iux} f_X(x)\, dx, \quad u \in \mathbb{R}, \tag{2.1.1}$$

where $f_X(x)$ is the probability density function of X.

The characteristic function is the expectation of e^{iux} and defines the probability distribution of a random variable. Note also that the characteristic function, apart from a factor $1/\sqrt{2\pi}$, corresponds to the Fourier transform in the continuous case. Moreover, it follows by

$$|\mathbb{E}(e^{iuX})| \leq \mathbb{E}|e^{iuX}| = \mathbb{E}(1) = 1, \tag{2.1.2}$$

that the characteristic function exists for all u and for all random variables, see [8].

Theorem 1. *Let X be a random variable. Then*

$$(a)\;\; |\varphi_X(u)| \leq \varphi_X(0) = 1; \tag{2.1.3}$$

$$(b)\;\; \overline{\varphi_X(u)} = \varphi_X(-u), \;\; \textit{where } \overline{\varphi_X(u)} \textit{ is the conjugate;} \tag{2.1.4}$$

$$(c)\;\; \varphi_X(u) \textit{ is (uniformly) continuous.} \tag{2.1.5}$$

Theorem 2. *Let X be a Gaussian random variable with expectation μ and standard deviation σ. Then the characteristic function for X is given by*

$$\varphi_X(u) \;=\; e^{i\mu u - \frac{1}{2}\sigma^2 u^2}. \tag{2.1.6}$$

Theorem 3. *Let $X_i, i = 1, 2, .., n$, be independent random variables and set $S_n = X_1 + ... + X_n$. Then the characteristic function for the sum S_n is given by*

$$\varphi_{S_n}(u) = \prod_{k=1}^{n} \varphi_{X_k}(u). \tag{2.1.7}$$

Theorem 4 (Fubini-Tonelli)**.** *Let X and Y be σ-finite measurable spaces. If f is a measurable function such that any one of the three integrals*

$$\int_X \left(\int_Y |f(x,y)|\, dy \right) dx, \quad \int_Y \left(\int_X |f(x,y)|\, dx \right) dy,$$

$$\iint_{X\times Y} |f(x,y)|\, d(x,y)$$

is finite, then they are all finite and

$$\int_X \left(\int_Y f(x,y)\, dy \right) dx = \int_Y \left(\int_X f(x,y)\, dx \right) dy = \iint_{X\times Y} f(x,y)\, d(x,y).$$

2.2 Basics in financial modeling

The theory behind finance enables us to study asset pricing on financial markets in continuous time. The purpose is to model assets as continuous stochastic processes using diffusion processes, stochastic differential equations and Martingale theory. The mathematical background can be heavy and we only introduce a small part of it. The purpose of this section is to give the reader an intuition about financial modeling. A more formal treatment can be found in [3].

A derivative is a financial contract whose value commonly depends on the price X_t at time t of an underlying asset. Our aim is to model the stochastic process $\{X_t\}_{t\geq 0}$ in order to price the financial contract. We say that X is a diffusion if its local dynamics can be approximated by a stochastic difference equation (SDE) of the type

$$X_{t+\Delta t} - X_t \;=\; \mu(t, X_t)\Delta t + \sigma(t, X_t)Z_t, \tag{2.2.1}$$

where μ and σ are deterministic functions and Z_t is a normally distributed noise-term independent of every event up to time t. We can think that the asset price over

the time interval $[t, t+\Delta t]$ is driven by two separate terms; one which is dependent on μ and determines the level of X, and one which is a Gaussian disturbance amplified by the factor $\sigma(t, X_t)$. We call functions μ and σ the (local) drift term and the diffusion term, respectively. The way we model the noise-term $Z(t)$ is by a Wiener process which is also known as a standard Brownian motion.

Definition 2. (Wiener process) *A stochastic process W is called a Wiener process if the following holds.*

i) $W(0) = 0$.

ii) *The process has independent increments, i.e. $W(t_2) - W(t_1)$ and $W(s_2) - W(s_1), 0 < s_1 < s_2 < t_1 < t_2$, are independent random variables.*

iii) $W(t) - W(s), 0 < s < t$, *has the Gaussian distribution* $N(0, t-s)$.

iv) W *has continuous trajectories.*

Since the Wiener process is unbiased, has zero expectation and has independent increments, it is suitable for modeling the noise-term Z_t which is the random driving force in financial modeling and we can replace Z_t with $\Delta W_t = W(t+\Delta t) - W(t)$, see [3]. By letting Δt tend to zero, i.e. making the expression in (2.2.1) more precise, we obtain the following stochastic differential equation (SDE)

$$\begin{aligned} dX_t &= \mu(t, X_t)dt + \sigma(t, X_t)dW_t, \\ X_0 &= x_0, \end{aligned} \tag{2.2.2}$$

which is actually shorthand for the integral equation

$$X_t = x_0 + \int_0^t \mu(s, X_s)ds + \int \sigma(s, X_s)dW_s. \tag{2.2.3}$$

The dynamics of the price process $\{X\}$ is determined by the SDE in equation (2.2.2), by which we define different asset price models, e.g. the ones in Chapter 4.

2.3 Valuation theory

Consider again a derivate which is dependent of the stochastic process $\{X_t\}_{t\geq 0}$. In valuation theory we let $(\Omega, \mathscr{F}^X, \mathscr{F}_t^X, \mathbb{P})$ be a filtered probability space on which $\{X_t\}$ is defined. We are then able to price derivatives using a well known-formula for asset pricing called the Risk Neutral Valuation Formula (RNVF).

Theorem 5. (Risk Neutral Valuation Formula) *The arbitrage free price of a contingent claim maturing at time T with contract function $\Phi(\cdot)$ is given by*

$$\pi(X_t) = p(t,T)\mathbb{E}^{\mathbb{Q}}[\Phi(X_T)|\mathscr{F}_t], \tag{2.3.1}$$

where the $\mathbb{Q}$-dynamics of X are those of equation (2.2.2).

Here $\mathscr{F}_t$ is a mathematical representation of the history of X. If X were to be discrete, the history up to time t would simply be the set

$$\{X_i, \quad i = 1, ..., t-1\},$$

making the conditional expectation in the RNVF well-defined (see p. 71-72 of [1]). For continuous processes however, greater care is required due to an infinite number of random variables and we therefore represent the history using a filtration.

Definition 3. (Filtration) *Consider a continuous stochastic process X on the time interval $[0, T]$. The filtration of X at time t is*

$$\mathscr{F}_t^X = \sigma(X_k : k \leq t), \tag{2.3.2}$$

where $\sigma(\bullet)$ denotes the smallest sigma-algebra generated by the set in $\bullet$.

An introduction to sigma algebras can be found in [14]. For the purpose of this thesis, it is enough to intuitively think of $\mathscr{F}_t^X$ as the historical information generated by X up to time t. We will from here-on refer to $\mathscr{F}_t$ as the *market filtration.*

2.4 The concept of parameter uncertainty

One flaw with the RNVF is the conditioning on the market filtration $\mathscr{F}_t$. In [11] the author argues that the model filtration is not available in real-life since the market suffers from imperfect information. The information which is actually observed by participants is the information generated by $\{X_t\}$ observed at discrete time points $t_1, t_2, ..., t_n$. We call it the *observed filtration* and it is defined by the following.

Definition 4. (Observed filtration) *The observed filtration of a stochastic process X at time t is*

$$\mathscr{F}_t^{Obs} = \sigma(X_{t_k}, \forall t_k \leq t), \tag{2.4.1}$$

where σ is the smallest sigma algebra generated by the set $\{X_{t_k}, \forall t_k \leq t\}$.

We note that since the set $\{X_{t_k}, \forall t_k \leq t\}$ is contained in the continuous set $\{X_k, \forall k \leq t\}$, this implies

$$\mathscr{F}^{Obs} \subseteq \mathscr{F}_t^{Market},$$

which we will use later on with the following theorem.

Theorem 6. (Tower property) *Let X be a r.v. and suppose $\mathscr{F}_1 \subseteq \mathscr{F}_2$ is a sub-σ-algebra. Then*

$$\mathbb{E}[X|\mathscr{F}_1] \; = \; \mathbb{E}[\mathbb{E}[X|\mathscr{F}_2]|\mathscr{F}_1]. \tag{2.4.2}$$

For now, let us exemplify the claim of imperfect information with an example: Investors form trading strategies based on different models. Since different participants have access to different data sets, they are likely to fit their model parameters

differently and in return obtain different theoretical option values. Some investors may therefore find a particular option expensive, while other investors find the opposite. An investor will typically buy when prices are low and sell when prices are high. The investors will therefore trade until they no longer consider the options mispriced, i.e. when the prices have stabilized somewhere in between their calibrated valuations.
In [2] it was shown that any valuation formula can be represented by a conditional expectation. This was later on used in [11] to show that the risk-neutral value of an option under the observed filtration can be written as

$$\begin{aligned}\tilde{\pi}(X_t) &= p(t,T)\mathbb{E}^{\mathbb{Q}}\left[\Phi(X_T)|\mathscr{F}_t^{Obs}\right] \\ &= p(t,T)\mathbb{E}^{\mathbb{Q}}\left[\mathbb{E}^{\mathbb{Q}}\left[\Phi(X_T)|\mathscr{F}_t\right]|\mathscr{F}_t^{Obs}\right] \\ &= \mathbb{E}^{\mathbb{Q}}[\pi(X_t)|\mathscr{F}_t^{Obs}], \end{aligned} \tag{2.4.3}$$

which is the projection of the $\mathscr{F}_t$-measurable value onto the set of $\mathscr{F}_t^{Obs}$-measurable values. Intuitively we may think of it as an average over different option values. The second equality followed from the tower property in (2.4.2).
It is also shown in [2] that parametric models generate risk-neutral distribution conditional on a filtration and fixed parameters θ_0. This distribution is used in all parametric valuation and we denote the obtained value by $\pi(t, X_t|\theta_0)$. The problem we experienced in the above example is that parameters are not known without errors and one should therefore take parameter uncertainty into account. This was done in [11] by interpreting parameters as a random vector θ. In the end, we arrive at

$$\tilde{\pi}(X_t) = \mathbb{E}^{\mathbb{Q}}[\pi(X_t|\theta)|\mathscr{F}_t^{Obs}], \tag{2.4.4}$$

which is the risk-neutral valuation formula under parameter uncertainty. It was found in [11] that the empirical performance of (2.4.4) is generally superior to the classic RNVF in (2.3.1).

2.5 Valuation using Fourier methods

Fourier methods hold nice properties such as being fast, accurate and applicable to a wide range of models, see [9]. We present the general idea behind option valuation using Fourier transforms. A more detailed review can be found in e.g. [5] and [15].

Let $\{S_t\}_{t\geq 0}$ be the stochastic price process of a stock. Furthermore, let $C(T,K)$ denote a European call option maturing at time T with strike price K. By definition this means that the holder of the European call has the option to buy the stock for the predefined price K at the predefined time T. From this we see that the payoff is a function given by

$$\max(0, S_T - K) = \begin{cases} S_T - K, & \text{if } S_T > K, \\ 0, & \text{otherwise.} \end{cases} \tag{2.5.1}$$

It is often convenient to consider the logarithm of prices and therefore we introduce the notation $s_t = \log(S_t)$ and $k = \log(K)$. The payoff is then given by

$$(e^s - e^k)\mathbb{I}[s > k],$$

where $\mathbb{I}$ denotes the indicator function. Let $f_t = f(s_t|s_0)$ denote the risk-neutral density of s_t. Then, by definition, the characteristic function for s_t is given by

$$\varphi_t(u) \;=\; \mathbb{E}^{\mathbb{Q}}[e^{ius_t}] = \int_{-\infty}^{\infty} e^{ius} f_t(s)\, ds. \tag{2.5.2}$$

According to the RNVF, the desired value $C(T,k)$ of the European call option is given by

$$C(T,k) \;=\; e^{-rT} \int_k^{\infty} (e^s - e^k) f_T(s)\, ds,$$

where we note that $C(T,k)$ is a non-square-integrable function since

$$C(T,k) \to s_0, \quad k \to -\infty.$$

However, square-integrability is required by Parseval's theorem and we therefore consider the modified call price

$$c(T,k) \;=\; e^{\alpha k} C(T,k), \quad \alpha > 0,$$

seeing as the function is square-integrable on the real line $\mathbb{R}$.
Now let $\mathfrak{F}$ be the Fourier transform of the modified call price, i.e.

$$\mathfrak{F}(u) \;=\; \int_{-\infty}^{\infty} e^{iuk} c(T,k)\, dk. \tag{2.5.3}$$

It can then be shown that the option value can be computed numerically by

$$C(T,k) \;=\; \frac{e^{-\alpha k}}{2\pi} \Re \left[\int_{-\infty}^{\infty} e^{-iuk} \mathfrak{F}(u)\, du \right] \tag{2.5.4}$$

$$\;=\; \frac{e^{-\alpha k}}{\pi} \int_0^{\infty} \Re[e^{-iuk} \mathfrak{F}(u)]\, du, \tag{2.5.5}$$

where $\Re[\cdot]$ denotes the real part and

$$\mathfrak{F}(u) \;=\; \frac{e^{-rT} \varphi_T(u - (\alpha+1)i)}{\alpha^2 + \alpha - u^2 + iu(2\alpha+1)}. \tag{2.5.6}$$

The second equality follows from the fact that $C(T,k)$ is real, implying that $\mathfrak{F}(u)$ is odd in its imaginary part and even in its real part (a full derivation can be found in [5]). Thus, by inserting (2.5.6) into (2.5.5) and performing the integration, we are able to price $C(T,k)$ using Fourier transforms. This technique, which we will call the Fourier method, is applicable to a variety of models and is computationally inexpensive, since efficient quadrature methods or fast Fourier transforms (FFT) can be used to compute the integral.

Remark 1. *It is not obvious that the domain of a characteristic function may be extended from the real line to the complex plane. We can however assume this if the moment generating function exists, which will be the case for the models considered in this thesis (see [7]).*

Chapter 3

FAST VALUATION UNDER PARAMETER UNCERTAINTY

The concept of parameter uncertainty was introduced in Chapter 2, along with a description of the Fourier method for option valuation. The two are now combined, resulting in a fast method for option valuation under parameter uncertainty. The method is then applied on four stock price models, i.e. the Black&Scholes, Merton, Heston and Bates models.

3.1 Fourier methods under parameter uncertainty

Let $C(T,k)$ be he value of a European call option maturing at time T with strike price $k = \log(K)$. Recall from equation (2.4.4) that the value of $C(T,k)$ under parameter uncertainty is given by

$$\tilde{C}(T,k) \;=\; \mathbb{E}^{\mathbb{Q}}[C(T,k|\theta)|\mathscr{F}_t^{Obs}]. \tag{3.1.1}$$

Our aim is to value $\tilde{C}(T,k)$ using the Fourier method since it is computationally inexpensive. If the characteristic function for $s_t = \log(S_t)$ was well-defined, then from (2.5.5) we found that the option value could be computed by

$$C(T,k) \;=\; \frac{e^{-\alpha k}}{\pi}\int_0^\infty \Re[e^{-iuk}\mathfrak{F}(u)]\,du, \tag{3.1.2}$$

where

$$\mathfrak{F}(u) \;=\; \frac{e^{-rT}\varphi_T(u-(\alpha+1)i)}{\alpha^2+\alpha-u^2+iu(2\alpha+1)}. \tag{3.1.3}$$

Combining the two above results gives us the following:

$$\begin{aligned}\tilde{C}(T,k) \;&=\; \mathbb{E}[C(T,k)|\mathscr{F}^{obs}] = \int_{\theta=-\infty}^{\infty} C(T,k|\theta)f(\theta)\,d\theta \\ &=\; \frac{e^{-\alpha k}}{\pi}\int_{\theta=-\infty}^{\infty}\int_{u=0}^{\infty} \Re[g(u)\cdot\varphi_T(u-(\alpha+1)i)\cdot f(\theta)]\,du\,d\theta, \end{aligned}\tag{3.1.4}$$

where

$$g(u) \;=\; \frac{e^{-rT}e^{-iuk}}{\alpha^2+\alpha-u^2+iu(2\alpha+1)}. \tag{3.1.5}$$

In order to compute $\tilde{C}(T,k)$ we need to change the order of integration in (3.1.4), something that is not given from a mathematical point of view. However, as the following proposition will show, we may actually do so.

Proposition 1. *Let k denote the logarithm of the strike price and let r, T and $\alpha > 0$ be constants. Let h denote the integrand*

$$h(u,\theta) \;=\; g(u)\cdot\varphi_T(u-(\alpha+1)i)\cdot f(\theta),$$

where φ_T is a characteristic function, $f(\theta)$ a probability density function and $g : \mathbb{R}\to\mathbb{C}$ is a function defined by

$$g(u) \;=\; \frac{e^{-rT}e^{-iuk}}{\alpha^2+\alpha-u^2+iu(2\alpha+1)}. \tag{3.1.6}$$

Then

$$\int_{\theta=-\infty}^{\infty}\left(\int_{u=0}^{\infty}h(u,\theta)\,du\right)d\theta \;=\; \int_{u=0}^{\infty}\left(\int_{\theta=-\infty}^{\infty}h(u,\theta)\,d\theta\right)du. \tag{3.1.7}$$

Proof. We recall that the characteristic function is bounded by 1, and therefore

$$|\varphi_T(u-(\alpha+1)i)| \;=\; |e^{\alpha+1}\varphi_T(u)| \le e^{\alpha+1}. \tag{3.1.8}$$

Since f is a PDF i.e. a positive function it follows that

$$|h(u,\theta)| \;\le\; e^{\alpha+1}|f(\theta)|\cdot|g(u)| \le e^{\alpha+1}f(\theta)|g(u)|. \tag{3.1.9}$$

Furthermore

$$\begin{aligned}|g(u)| \;&=\; \frac{|e^{-rT}e^{-iuk}|}{|\alpha^2+\alpha-u^2+iu(2\alpha+1)|} \le \frac{e^{-rT}}{|(iu+\alpha+1)(iu+\alpha)|}\\ &=\; \frac{e^{-rT}}{\sqrt{(u^2+[\alpha+1]^2)(u^2+\alpha^2)}} \le \frac{e^{-rT}}{\sqrt{(u^2+\alpha^2)(u^2+\alpha^2)}}\\ &=\; \frac{e^{-rT}}{u^2+\alpha^2}.\end{aligned} \tag{3.1.10}$$

We note that

$$u^2+\alpha^2 \ge \alpha^2 > 0$$

since we assume $\alpha > 0$. Most importantly, we note that $|g|$ behaves like $1/u^2$ for large u and is bounded, from which it follows that $|g|$ is integrable on $\mathbb{R}$.

Since both f and g are integrable in the variables θ and u, respectively, it follows from the estimate (3.1.9) that

$$\int_{\theta=-\infty}^{\infty}\int_{u=0}^{\infty} |h(u,\theta)|\,du\,d\theta \;<\; \infty,$$

and we can apply the Fubini-Tonelli theorem in Theorem 4. Thus

$$\int_{\theta=-\infty}^{\infty}\left(\int_{u=0}^{\infty} h(u,\theta)\,du\right)\,d\theta \;=\; \int_{u=0}^{\infty}\left(\int_{\theta=-\infty}^{\infty} h(u,\theta)\,d\theta\right)\,du \qquad (3.1.11)$$

□

It follows from Proposition 1 that the desired option value under parameter correction can be computed with the Fourier method by

$$\tilde{C}(T,k) \;=\; \frac{e^{-\alpha k}}{\pi}\int_{u=0}^{\infty} g(u)\left(\int_{\theta=-\infty}^{\infty} \varphi_T(u-(\alpha+1)i)\cdot f(\theta)\,d\theta\right)\,du, \quad (3.1.12)$$

giving us a fast method for valuation under parameter uncertainty. However, there are two restrictions to the method. First of all, we require the characteristic function φ to be well-defined in the applied model. Secondly, we also need to ensure that the integral

$$\tilde{\varphi}_\theta(u) \;:=\; \int_{\theta=-\infty}^{\infty} \varphi_T(u-(\alpha+1)i)\cdot f(\theta)\,d\theta \qquad (3.1.13)$$

is in itself a characteristic function, which we will call the modified characteristic function. A formal proof that $\tilde{\varphi}$ is a characteristic function is not available at the moment, but we can motivate this for exponentially affine characteristic functions. We show this explicitly for the stock price models in the next section.

3.2 Application on stock price models

The method described in Section 3.1 is applied on four common stock price models in contemporary literature, i.e the Black&Scholes (1973), Merton (1976), Heston (1993) and Bates (1996) models. In order to use equation (3.1.12) we need to ensure that the expression in (3.1.13) can be seen as a new characteristic function. We motivate that this should hold for exponentially affine characteristic functions.

3.2.1 The Black&Scholes model

In 1973 Black and Scholes published a paper on option pricing under the assumption of no arbitrage opportunities. Under the risk-neutral measure $\mathbb{Q}$ the stochastic price process S_t is modelled by

$$dS_t \;=\; rS_t dt + \sigma S_t dW_t, \quad S_0 = s, \qquad (3.2.1)$$

where r is the short risk-free rate and σ is the (constant) diffusion term. $S_0 = s$ is the initial price. The Ito formula provides us with a solution to (3.2.1) given by

$$S_t \;=\; S_0 \exp[(r - \tfrac{\sigma^2}{2})t + \sigma W_t], \tag{3.2.2}$$

where W_t is a Wiener process with Gaussian distribution $N(0,t)$. Then the distribution of $s_t = \log(S_t)$ is given by

$$N(s_0 + [r - \tfrac{\sigma^2}{2}]t, \sigma^2 t).$$

By Theorem 2 the characteristic function for s_t is given by

$$\varphi(u) \;=\; \exp[i(us_0 + (r - \tfrac{\sigma^2}{2})t)u - \tfrac{1}{2}\sigma^2 t u^2]. \tag{3.2.3}$$

We note that the characteristic function is exponentially affine [1] in $\theta = \sigma^2$, making it easy to compute the modified characteristic function $\tilde{\varphi}$. By inserting (3.2.3) into (3.1.13) we obtain

$$\tilde{\varphi}_\theta(u) \;=\; e^{iu(s_0+rT)} \int_{\theta=-\infty}^{\infty} e^{i\theta\frac{T}{2}(-u+iu^2)} \cdot f(\theta)\, d\theta, \tag{3.2.4}$$

which is the modified characteristic function for the parameter $\theta = \sigma^2$ in the Black-Scholes model. We note that the form of $\tilde{\varphi}_\theta$ is the same as of a characteristic function evaluated in the point $\frac{T}{2}(-u + iu^2)$, apart from a factor $e^{iu(s_0+rT)}$. We should therefore be able to regard $\tilde{\varphi}$ as a characteristic function. We are then able to value options with uncertainty in σ^2.

3.2.2 The Merton model

The Merton model extends the Black-Scholes model by adding a simple jump process, called a Poisson process, to the stock price dynamics. This enables us to model sudden and unexpected price jumps. But first, we introduce some definitions from [8].

Definition 5. (Poisson process) *A Poisson process is a nonnegative, integer-valued stochastic process* $\{N(t), t \geq 0\}$ *such that*

- (*a*) $N(0) = 0$;
- (*b*) *the increments* $\{N(t_k) - N(t_{k-1}), 1 \leq k \leq n\}$ *are independent random variables for all* $0 \leq t_0 \leq t_1 \leq ... \leq t_{n-1} \leq t_n$ *and all* n;
- (*c*) *there exists a* $\lambda > 0$, *called the intensity, such that* $N(t) - N(t') \in Po(\lambda(t - t')), \quad 0 \leq t' \leq t.$

[1] i.e. can be written as a function $f(x_1, x_2, ...) = \exp\{a_1x_1 + a_2x_2... + b\}$

Definition 6. (Compound Poisson process) *A compound Poisson process is defined as*

$$Z(t) \;=\; \sum_{n=0}^{N(t)} Y_n, \tag{3.2.5}$$

where $N(t)$ is a Poisson process and $\{Y_n, n \in \mathbb{N}\}$ are i.i.d. random variables independent of N.

The compound Poisson process contains two sources of randomness: one originating from $N(t)$ which causes the asset price to jump randomly and one originating from the random variables Y_n, determining the jump sizes. In order to model sudden and unexpected jumps, all random parts are assumed to be independent of each other. The only difference between the BS and Merton model is the addition of the compound Poisson process.
The stock price dynamics are modelled by

$$dS_t = \mu S_t dt + \sigma S_t dW_t + S_t dZ_t, \quad S_0 = s, \tag{3.2.6}$$

where Z_t is a compound Poisson process with jump intensity λ and log-normally distributed jumps, $Y_n \sim LN(\mu, \delta^2)$. The exact solution to (3.2.6) is given by

$$S_t \;=\; s \exp\left(\tilde{\mu} t + \sigma W_t + \sum_{n=0}^{N(t)} Y_n\right), \tag{3.2.7}$$

where $\tilde{\mu} = r - \frac{\sigma^2}{2} - \lambda(\exp[\mu + \frac{\delta^2}{2}] - 1)$. Since the exponent is a sum of random variables we can use Theorem 3 to find the characteristic function for s_t, which is given by

$$\varphi(u) \;=\; \exp\left[i(s_0 + \tilde{r}T)u - \tfrac{\sigma^2 u^2 T}{2} + \lambda T(e^{i\mu u - \frac{\delta^2 u^2}{2}} - 1)\right], \tag{3.2.8}$$

$$\tilde{r} \;=\; r - \tfrac{\sigma^2}{2} - \lambda(\exp[\mu + \tfrac{\delta^2}{2}] - 1). \tag{3.2.9}$$

As with the Black-Scholes model, we can insert the characteristic function in (3.2.8) into (3.1.13) in order to find the modified characteristic function $\tilde{\varphi}$. It is found to be exponentially affine in the jump intensity λ and the variance σ^2. We therefore only add correction into those parameters. Doing so, and then breaking out all factors that do not depend on the uncertain parameter, we obtain the following modified characteristic functions:

$$\tilde{\varphi}_\lambda \;=\; e^{iu(s_0 + (r - \frac{\sigma^2}{2})T) - \frac{\sigma^2 u^2 T}{2}} \int_{\lambda=-\infty}^{\infty} e^{i\lambda g(u)} \cdot q(\lambda)\, d\lambda, \tag{3.2.10}$$

$$\tilde{\varphi}_{\sigma^2} \;=\; e^{h_1(u)} \int_{\sigma^2=-\infty}^{\infty} e^{i\sigma^2 h(u)} \cdot q(\sigma^2)\, d\sigma^2, \tag{3.2.11}$$

where

$$g(u) = -T[u(e^{\mu+\frac{\delta^2}{2}}-1)+i(e^{i\mu u-\frac{\delta^2 u^2}{2}}-1)], \tag{3.2.12}$$

$$h_1(u) = iu(s_0+(r-\lambda[e^{\mu+\frac{\delta^2}{2}}-1])T)+\lambda T(e^{i\mu u-\frac{\delta^2 u^2}{2}}-1), \tag{3.2.13}$$

$$h_2(u) = -T(iu+u^2)/2. \tag{3.2.14}$$

3.2.3 The Heston model

The Black-Scholes and Merton models assumes the volatility is given by a deterministic function. Modeling the volatility as a stochastic process $\{v_t\}$, on the other hand, has shown to be more true to real-life observations. In 1996 Heston modelled the dynamics of S_t as a Wiener process with stochastic variance. Under the risk-neutral measure $\mathbb{Q}$, the dynamics are given by

$$\begin{aligned} dS_t &= rS_t dt+\sqrt{v_t}S_t dW_t^S, \\ dv_t &= \kappa(\Theta-v_t)dt+\eta\sqrt{v_t}dW_t^v, \end{aligned}$$

where v_0 is the initial variance, η is the volatility of volatility and θ is the long variance, meaning that the expected value of v_t will tend to θ as t tends to infinity. κ is called the speed of mean reversion and measures the rate at which v_t reverts to θ. The diffusion terms W_t^S, W_t^v are Brownian motions with with correlation ρ. Typically, ρ is negative which means that the volatility tends to increase when returns are negative, known as the leverage effect. Moreover, if the Feller condition

$$2\kappa\theta > \eta^2$$

holds, then the process $\{v_t\}_{t>0}$ is strictly positive.
In the Heston model, the characteristic function for s_t can be shown to follow (see Schoutens et al., 2004 or Heston, 1993)

$$\varphi(u) = \exp[A(u)+\Theta B(u)+V_0 C(u)],$$

where

$$A(u) = iu(s_0+rT), \tag{3.2.15}$$

$$B(u) = \tfrac{\kappa}{\eta^2}\left[(\kappa-\rho\eta iu-d)T-2\ln\left(\tfrac{(\kappa-i\rho\eta u)(1-e^{-dT})+d(e^{-dT}+1)}{2d}\right)\right], \tag{3.2.16}$$

$$C(u) = \frac{(1-e^{-dT})(-iu-u^2)}{(\kappa-i\rho\eta u)(1-e^{-dT})+d(e^{-dT}+1)}, \tag{3.2.17}$$

$$d = \sqrt{(\rho\eta iu-\kappa)^2+\eta^2(iu+u^2)}. \tag{3.2.18}$$

We notw that $\varphi(u)$ is exponentially affine in the initial variance v_0 and long variance Θ. Inserting $\varphi(u)$ into (3.1.13) we obtain the modified characteristic functions

$$\tilde{\varphi}_{V_0} = e^{A(u)+B(u)}\int_{V_0=-\infty}^{\infty} e^{V_0 C(u)}\cdot q(V_0)\,dV_0, \tag{3.2.19}$$

$$\tilde{\varphi}_{\Theta} = e^{A(u)+C(u)}\int_{\Theta=-\infty}^{\infty} e^{\Theta B(u)}\cdot q(\Theta)\,d\Theta, \tag{3.2.20}$$

from which we see that we may break ut an imaginary unit i in the exponent of the integrand in order to obtain the usual appearance of a characteristic function.

3.2.4 The Bates model

The Bates model combines the Merton and Heston models, adding jumps to the stock price dynamics of Heston. The dynamics under $\mathbb{Q}$ are given by

$$\begin{aligned} dS_t &= rS_t dt + \sqrt{v_t} S_t dW_t^S + dZ_t, \\ dv_t &= \kappa(\theta - v_t)dt + \eta\sqrt{v_t} dW_t^v, \end{aligned}$$

where ρ is the covariance of W_t^S, W_t^V. Here Z_t is a compound Poisson process with jump intensity λ and independent jumps $\{J_t\}_{t\geq 0}$ such that

$$\ln(1+J_t) \in N\left(\ln[1+\mu_J] - \tfrac{\sigma_J^2}{2}, \sigma_J^2\right),$$

with parameters μ_J and σ_J^2. Furthermore, the Poisson process is assumed to be independent of the Wiener processes.
It can be shown that the characteristic function for s_t is given by

$$\varphi(u) = \exp[A(u) + \Theta B(u) + V_0 C(u) + \lambda D(u)],$$

where the coefficients $A(u), B(u), C(u)$ are identical to the those in the Heston model, see equations (3.2.15) to (3.2.17). The term $D(u)$ is given by

$$D(u) = T\left[-\mu_J iu + (1+\mu_J)^{iu} \exp\left(\tfrac{\sigma_J^2(-u^2-iu)}{2}\right) - 1\right]. \tag{3.2.21}$$

The characteristic function is affine in parameters v_0, Θ and λ and thus we obtain the following modified characteristic functions:

$$\tilde{\varphi}_{V_0} = e^{A(u)+B(u)+D(u)} \int e^{V_0 C(u)} \cdot q(V_0)\, dV_0, \tag{3.2.22}$$

$$\tilde{\varphi}_{\Theta} = e^{A(u)+C(u)+D(u)} \int e^{\Theta B(u)} \cdot q(\Theta)\, d\Theta, \tag{3.2.23}$$

$$\tilde{\varphi}_{\lambda} = e^{A(u)+B(u)+C(u)} \int e^{\lambda D(u)} \cdot q(\lambda)\, d\lambda. \tag{3.2.24}$$

As in the Heston model, we can break out the imaginary unit to obtain the usual appearance of a characteristic function.

We have thus shown that parameter uncertainty (or parameter corrections) can be derived within the Fourier framework, for some parameters in the above models. The requirement is that the parameter of interest is exponantially affine in the characteristic function. The models having a correction in a parameter (within the Fourier framework) will from here-on be referred to as *corrected* or *modified* models.

Chapter 4

SIMULATION STUDY

The valuation formula derived in Section 3.1 is used to simulate call options for different strikes and maturities. This makes it possible for us to study if the corrected models in Section 3.2 are able to capture tendencies perceived from empirical observations. The volatility implied by the market, called implied volatility, will be considered here since it is a more useful measure of an options relative value than the actual option price.
The theorethical value of an option is typically a function of the volatility. Given an option value, the implied volatility can be extracted by inverting the function. The function considered here is the B&S pricing formula given by

$$\begin{aligned} C(\tau, K) &= N(d_1)S - N(d_2)Ke^{-r\tau}, \\ d_1 &= \frac{1}{\sigma\sqrt{\tau}}[\ln(S/K) + \tau(r + \sigma^2/2)], \\ d_2 &= \frac{1}{\sigma\sqrt{\tau}}[\ln(S/K) + \tau(r - \sigma^2/2)], \end{aligned}$$

where $N(\cdot)$ is the cumulative distribution function of the standard Gaussian distribution, S is the spot price, K is the strike, τ is time to maturity and r is the interest rate. Since the price is a monotone increasing function of the volatility, the Bisection method was implemented with tolerance level 10^{-7} (see chapter 2 in [4]) in order to obtain the implied volatilities.
The non-corrected B&S model assumes constant volatility, i.e the implied volatility does not depend on the strike level or time to maturity and we should expect the implied volatility surface to be flat. On most markets however, we can depict a skew in the surface called volatility smile. This makes the B&S model incompatible with market data and one will usually have to turn to more complex models in order to obtain the smile. In the simulation study we will see that adding a correction in the volatility will give rise to a volatility smile even for the B&S model. A comparison with [11], where Monte-Carlo methods were used rather than Fourier methods, shows consistent results for the B&S and Merton models. We keep in mind that the computational complexity using the Fourier method is $\mathcal{O}(n)$ which is an improvement over the Monte Carlo technique used in the paper which has a computational complexity of $\mathcal{O}(nK)$, where K is the number of Monte Carlo

samples. Another disadvantage with the Monte Carlo technique is its inability to sample from more advanced models such as the Heston and Bates models.

4.1 Implementation of the Fourier method

The modified characteristic functions $\tilde{\varphi}$ were solved analytically in Chapter 3.2. Options were then valued in MATLAB using fast Fourier transforms for different strikes and maturities on equally spaced grids. We consider only the real part since any price is a real number.
In order to avoid using different grids for different strikes and maturities, a Gauss-Laguerre quadrature impementation was used for the inverse Fourier transformations. The Gauss-Laguerre quadrature formula approximates an exponentially weighted integral from zero to infinity as

$$\int_{x=0}^{\infty} e^{-x} f(x)\, dx \approx \sum_{i=1}^{n} w_i f(x_i), \tag{4.1.1}$$

where x_i is the i-th root of the Laguerre polynomial. This thesis uses $n = 500$. The integration was improved by optimizing over the α-parameter needed to make the option values square-integrable. The α-parameter was chosen in order to reduce unwanted oscillations in the characteristic function, see [13].

The market is simulated with inital stock price $s_0 = 100$, strike levels $K = 80, ..., 120$ in steps of $\Delta K = 2$ and time to maturity $\tau = 0.1, ..., 2$ in steps of $\Delta\tau = 0.1$. The interest-free rate is $r = 0.04$. For simplicity, all uncertain parameters were assumed to be uniformly distributed in the interval $[a, b]$, $a < b$. The a- and b-parameters were chosen such that the expectation is 0.2 for volatilities and 2 for jump intensities.

Remark 2. *The uniform distribution was chosen for simplistic reason and for the advantage of dealing with a compact support (for the density function). For the volatility, the log-ormal or χ^2 would be more reasonable distributions. One may even suggest the Gaussian distribution if the variance is small, seeing as the asymptotic distribution for most estimates is Gaussian by the Central Limit theorem (CLT).*

4.2 Black & Scholes

We add uncertainty to the variance i.e. we let $\theta = \sigma^2$. The variance is assumed to follow the uniform distribution $\mathrm{U}(a, b)$ and we are thus able to finish the analytical comuptation of the modified characterstic function in (3.2.4) by the following.

$$\begin{aligned} \tilde{\varphi}_{\sigma^2} &= \frac{e^{iu(s_0+rT)}}{b-a} \int_{\theta=a}^{b} e^{-\theta\frac{T}{2}(iu+u^2)}\, d\theta \\ &= \frac{e^{iu(s_0+rT)}}{b-a} \cdot \frac{(e^{cb} - e^{ca})}{c}, \end{aligned} \tag{4.2.1}$$

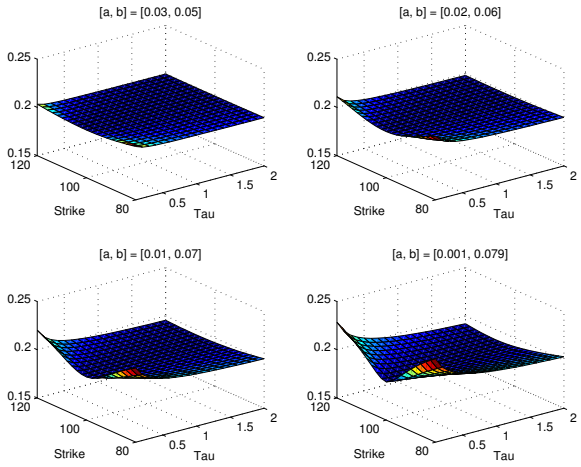

Figure 4.1: **(Black-Scholes)** Implied volatility in the corrected model for increasing level of parameter uncertainty, i.e. wider interval $[a, b]$ in the uniform distribution.

where $c = -\frac{T}{2}(iu + u^2)$ and $u = v - (\alpha + 1)i$. The modified characteristic function is then used in the implementation of the Fourier method.
The resulting implied volatilities using

$$[a, b] = [0.03, 0.05], [0.02, 0.06], [0.01, 0.07], [0.001, 0.079]$$

are shown in Figure 4.1. It can be seen that large parameter uncertainty generates a significant volatility smile which is consistent with empirical observations.

Remark 3. *An additional study, where σ^2 is assumed to follow the triangular distribution Tri(a, b, c), is shown Appendix B. The resulting implied volatilities were similar to those in Figure 4.1. We find that it is the variance rather than the shape of the uncertainty that seems to matter.*

4.3 Merton

In Section 3.2.2 the variance σ^2 and jump intensity λ were found to be exponentially affine in the modified characterstic function and we are therefore to add uncertainty in these parameters. Uncertainty is added to one parameter at a time where we let remaining parameters have values: volatility $\sigma = 0.2$, jump intensity $\lambda = 2$, expected jump size $\mu_J = -0.1$ and jump size volatility $\sigma_J = 0.1$.
Completing the integrations in (3.2.10) and (3.2.11) the modified characteristic

functions for σ and λ are given by

$$\tilde{\varphi}_\lambda = \frac{e^{iu(s_0+(r-\frac{\sigma^2}{2})T)-\frac{\sigma^2 u^2 T}{2}}}{c_1(b-a)} \cdot (e^{c_1 b} - e^{c_1 a}), \tag{4.3.1}$$

$$c_1 = T(-iu(e^{\mu+\frac{\delta^2}{2}} - 1) + e^{i\mu u - \frac{\delta^2 u^2}{2}} - 1) \tag{4.3.2}$$

and

$$\tilde{\varphi}_{\sigma^2} = \frac{e^{iu(s_0+(r-\lambda[e^{\mu+\frac{\delta^2}{2}}-1])T)+\lambda T(e^{i\mu u-\frac{\delta^2 u^2 T}{2}}-1)}}{c_2(b-a)} \cdot (e^{c_2 b} - e^{c_2 a}), \tag{4.3.3}$$

$$c_2 = -\frac{T(iu+u^2)}{2}, \tag{4.3.4}$$

respectively. The resulting implied volatilities using

$$\begin{aligned} \sigma^2 &\sim U(a,b), \quad [a,b] = [0.19, 0.21],\ [0.15, 0.25],\ [0.1, 0.3],\ [0.01, 0.39], \\ \lambda &\sim U(a,b), \quad [a,b] = [1.99, 2.01],\ [1.9, 2.1],\ [1, 3],\ [0.8, 3.2], \end{aligned}$$

are shown in Figure 4.2. The surface differences are shown in Figure 4.3. We see that large uncertainty in σ^2 generates a volatility smile similar to the one in the B&S model, while it does not seem to generate a noticeable difference with uncertainty in λ. This is consistent with the findings in [11]. We may need to assign even larger uncertainty to λ in order to obtain a noticeable volatility skew.

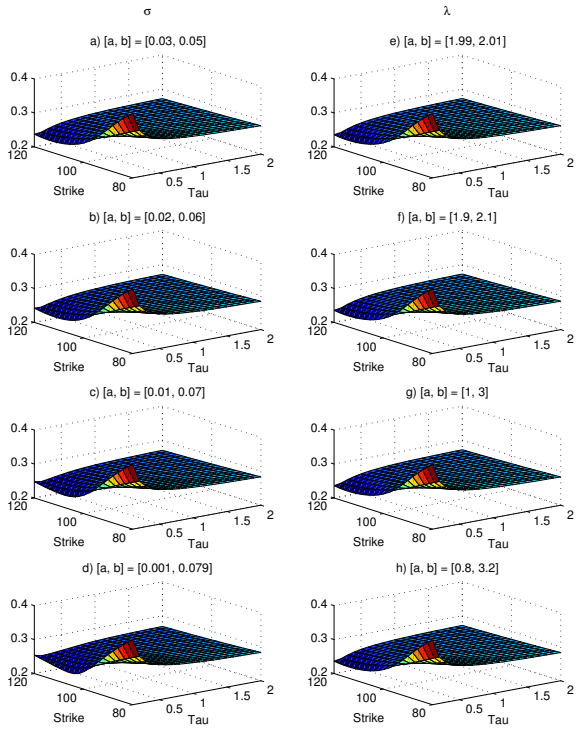

Figure 4.2: **(Merton)** Implied volatility in the corrected model for increasing level of parameter uncertainty, i.e. wider interval $[a, b]$ in the uniform distribution.

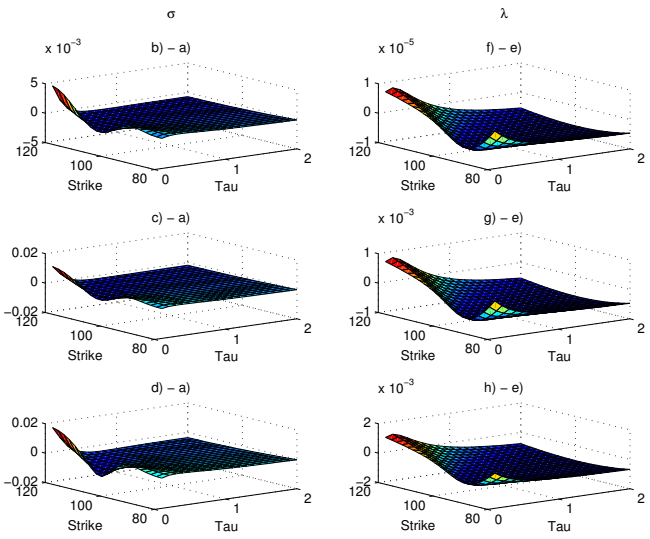

Figure 4.3: **(Merton)** Difference in implied volaility, cf. Figure 4.2.

4.4 Heston

The Heston model is parametrized by $\rho = -0.02, \eta = 0.2, \kappa = 2, \Theta = 0.04, V_0 = 0.04$. which is similar to parameters calibrated to S & P 500 index options. From (3.2.19) and (3.2.20) we obtain the modified characteristic functions

$$\tilde{\varphi}_{v_0} = \frac{e^{A(u)+B(u)}}{C(u)(b-a)}(e^{C(u)b} - e^{C(u)a}), \tag{4.4.1}$$

$$\tilde{\varphi}_{\Theta} = \frac{e^{A(u)+C(u)}}{B(u)(b-a)}(e^{B(u)b} - e^{B(u)a}), \tag{4.4.2}$$

for initial variance v_0 and long variance Θ, respectively, with koefficients A, B, C defined in equations (3.2.15) to (3.2.17).
The implied volatilities, assuming the uniform distribution $\mathrm{U}(a, b)$ where

$$[a, b] = [0.03, 0.05],\ [0.02, 0.06],\ [0.01, 0.07],\ [0.001, 0.079],$$

are shown in Figure 4.4. The general pattern is similar to the B&S and Merton models, seeing as the correction accentuates the short term volatility smile.
The difference in implied volatilities is shown in Figure 4.5, where we see a (weak) long term smile when applying correction to Θ. This is interesting as the implied volatility flattens out for most models due to a Central Limit Theorem type convergence in the transition kernel. The correction is therefore particularly useful if there is some long time volatility smile.

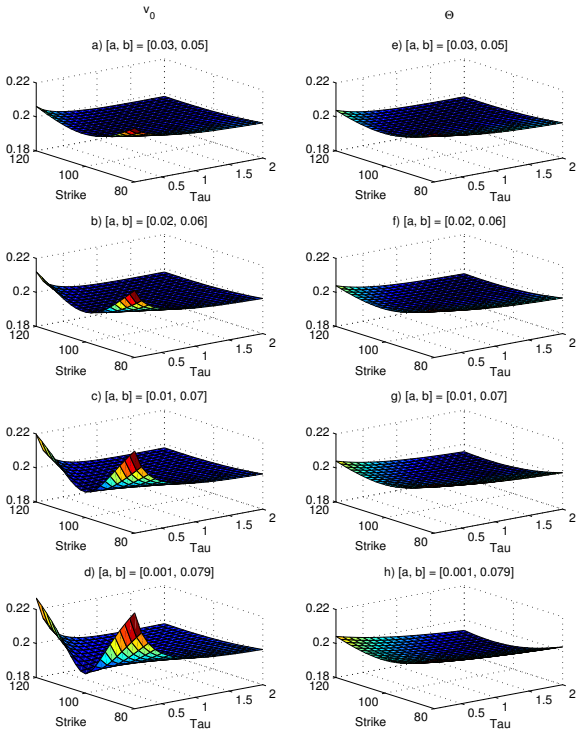

Figure 4.4: **(Heston)** Implied volatility in the corrected model for increasing level of parameter uncertainty, i.e. wider interval $[a, b]$ in the uniform distribution.

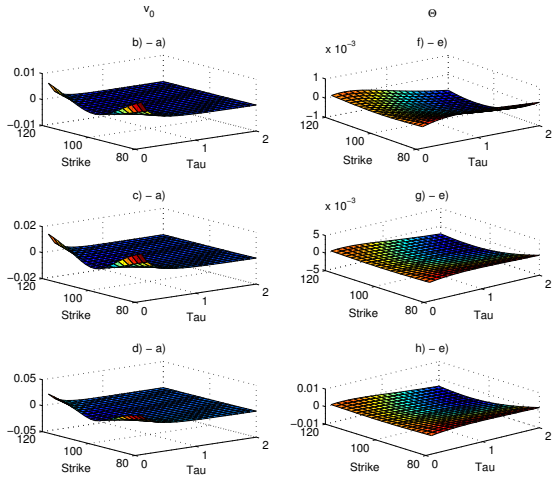

Figure 4.5: **(Heston)** Difference in implied volaility, cf. Figure 4.4.

4.5 Bates

The parameters of the Bates model were assigned the same values as in the Heston model with an added jump intensity of $\lambda = 2$, expected jump size $\mu_J = -0.1$ and jump size volatility $\sigma_J = 0.1$. From equations (3.2.22), (3.2.23) and (3.2.24) we obtain the following modified characteristic functions:

$$\tilde{\varphi}_{V_0} = \frac{e^{A(u)+B(u)+D(u)}}{C(u)(b-a)}(e^{C(u)b} - e^{C(u)a}), \tag{4.5.1}$$

$$\tilde{\varphi}_{\Theta} = \frac{e^{A(u)+C(u)+D(u)}}{B(u)(b-a)}(e^{B(u)b} - e^{B(u)a}), \tag{4.5.2}$$

$$\tilde{\varphi}_{\lambda} = \frac{e^{A(u)+B(u)+C(u)+}}{D(u)(b-a)}(e^{D(u)b} - e^{D(u)a}), \tag{4.5.3}$$

for initial variance v_0, long variance Θ and jump intensity λ. The resulting implied volatilities, using

$$\begin{aligned} V_0,\ \Theta &\sim U(a,b), \quad [a,b] = [0.03, 0.05],\ [0.02, 0.06],\ [0.01, 0.07],\ [0.001, 0.079], \\ \lambda &\sim U(a,b), \quad [a,b] = [1.99, 2.01],\ [1.9, 2.1],\ [1, 3],\ [0.8, 3.2], \end{aligned}$$

are shown in Figure 4.6 and Figure 4.7. Compared to the Heston model we can depict an even weaker volatilty smile with uncertainty in long term Θ. As in the Merton case, it seems as if we will have to add larger uncertainty to be able to depict a significant difference for the jump intensity.

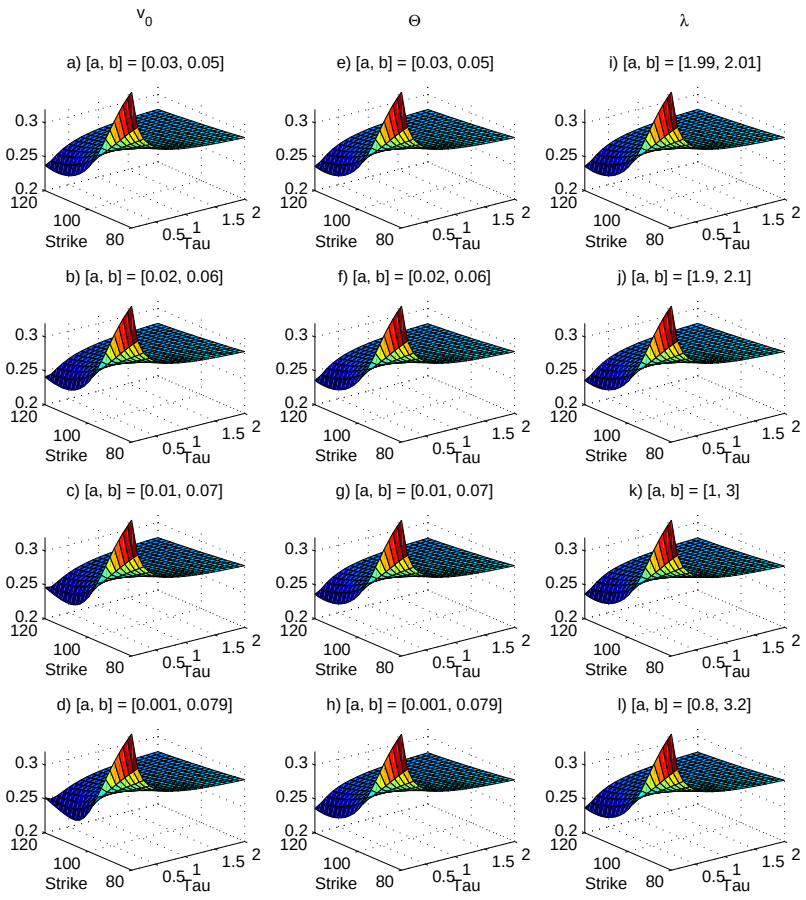

Figure 4.6: **(Bates)** Implied volatility in the corrected model for increasing level of parameter uncertainty, i.e. wider interval $[a, b]$ in the uniform distribution.

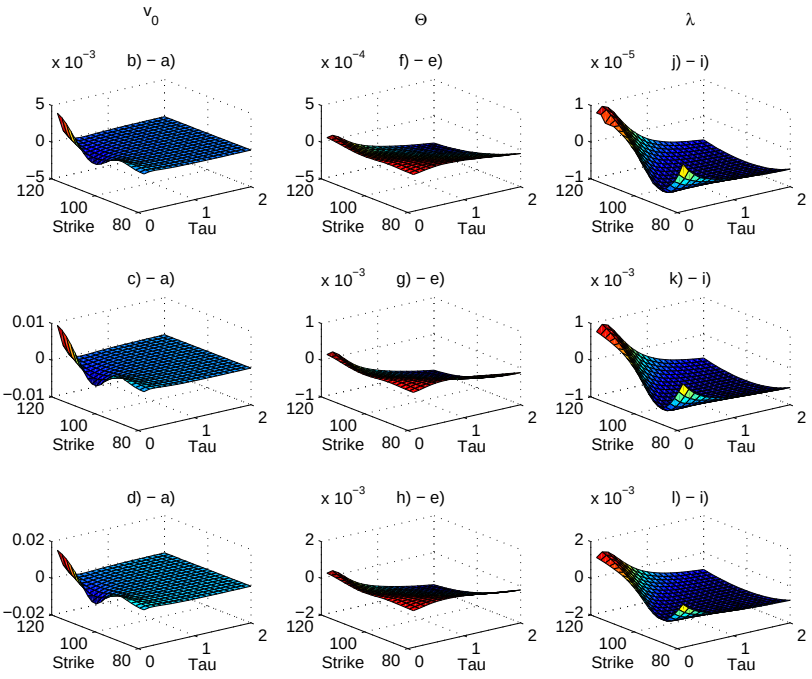

Figure 4.7: **(Bates)** Difference in implied volaility, cf. Figure 4.6.

Chapter 5

EMPIRICAL STUDY

The data set consists of daily S&P 500 index options from November 5th 2001 to May 5th 2003, excluding data containing short-term effect following September 11th. The raw data was processed by excluding outliers and ill-liquid quotes (details can be found in [13]). A total of 28394 unique quotes remained after the process which were allocated over 242 trading days. All quoted put options were for convenient reasons transformed into call options using the Put-Call parity. The continuously compounded short rate r was replaced by a zero-coupon bond yield as described in [13].
We compare the performance of corrected models and their standard counterparts using the Root-Mean-Square Error (RMSE). The RMSE measures the difference between the predicted values and the observed values, and is defined by

$$RMSE(\hat{\theta}) = \sqrt{\frac{1}{n}\sum_{i=1}^{N}(y_i - \hat{y}_i)^2}, \tag{5.0.1}$$

where y_i are the observed option prices and $\hat{y}_i$ is the estimated price under $\hat{\theta}$. The uncertain parameter is specified within brackets $[\theta]$ for each model. As in the simulation study, uncertain parameters are assumed to follow a Uniform distribution. The parameters are first estimated in sample, meaning that they are fitted to the observations. We then make predictions by the following procedure:
1. Fit the parameters to the observed quotes at the ith day.
2. Use the estimated parameters to predict prices for the next day, i.e day $i+1$.
3. Compute RMSE to measure the performance of prediction for each day.

5.1 Least Squares method

Model parameters are estimated using nonlinear least squares (LS) which minimizes the sum of squared differences between values predicted by the model and observed values:

$$\hat{\theta}_t = \arg\min_{\theta} \sum_{i=1}^{N} [C_t(K_i, \tau_i) - C_t^{Model}(K_i, \tau_i; \theta)]^2. \tag{5.1.1}$$

LS methods can be shown to give the best parameter fit in sample although they may suffer from numerical difficulty in the minimization problem, as discussed in [6]. The numerical difficulties can be reduced by adding the penalty

$$P(\theta) \;=\; \xi(\theta - \theta_{t-1})^T Q^{-1}(\theta - \theta_{t-1}), \tag{5.1.2}$$

where Q is the estimated covariance matrix of the parameters. For sufficiently large ξ, the LS estimator should be globally convex and prevents the parameter vector from getting caught in a local minimum.
The nonlinear LS minimization with added penalty function $P(\theta)$ was implemented using the MATLAB routine 'lsqnonlin'. For each model, the parameters were estimated for the first 50 trading days using $\xi = 0.01, 0.1, 1, 10, 100, 1000$. We then chose to fit the remaining quotes using the ξ-value that gave the lowest RMSE for that particular model. If several values gave rise to the same RMSE, ξ was chosen based on computation time.

5.1.1 Results

Black & Scholes

The estimated volatility σ in the B&S model is shown in Figure 5.1. The results for the corrected model is shown in 5.2. We see that a correction in σ is preferred since the estimated a- and b-parameters are far apart from each other in a majority of the trading days. We should therefore expect the corrected B&S to have lower RMSE than the standard B&S model. This is indeed the case in Figure 5.3. Returning to Figure 5.2, we note that the mean is conserved at approximately 0.2 and does not contradict the estimations in Figure 5.1.
The mean and median RMSE measuring predictive performance can be seen in Table 5.1. We can depict an improvement in both, particularly in the median which does not take outliers into account.

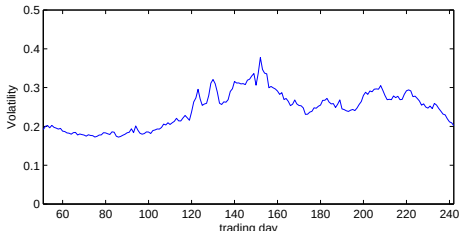

Figure 5.1: **(Black-Scholes)** Estimated volatility in sample.

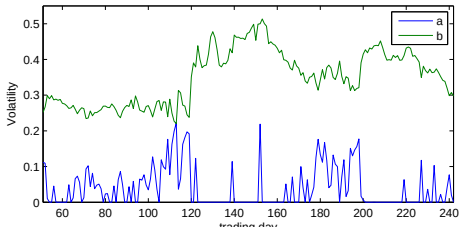

Figure 5.2: **(Black-Scholes** $[\sigma]$**)** Parameters a and b estimated in sample, where $\sigma \in U(a, b)$.

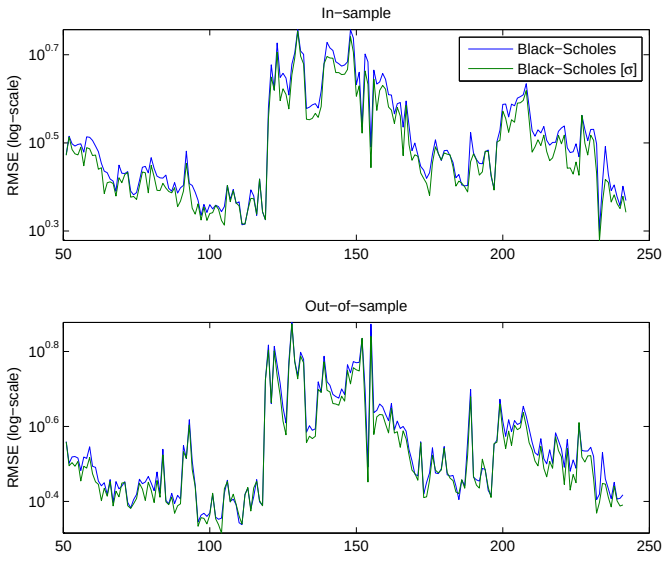

Figure 5.3: RMSE for estimation in sample and predictions.

In-sample

Model	Mean RMSE	Median RMSE
BS	3.2616	3.0392
BS $[\sigma]$	3.1051	2.9074

Out-of-sample

Model	Mean RMSE	Median RMSE
BS	3.5653	3.2406
BS $[\sigma]$	3.4301	3.0771

Table 5.1: Mean and median of RMSE for in-sample fit and predictions out of sample (day 50 to 246).

Merton

Estimated parameters in the Merton model is shown in Figure 5.4. The results with uncertainty in volatility σ and jump intensity λ can be seen in Figure 5.5 and Figure 5.6, respectively. Up to approximately day 120 the estimates support a correction in σ. Afterwhich, the model seems to struggle with keeping the parameters apart or even letting $a > b$. In the three mentioned figures, we also see a shift between σ and λ. The σ-parameter is close to zero (which is highly unlikely), something that the model seems to compensate by a large λ-parameter. A jump intensity of 20 jumps per unit is very odd and the Merton model does not seem able to capture the dynamics of the data. We can however depict some improvement in RMSE for Merton model with a correction in λ, see Figure 5.7. This suggests that the model is better at capturing the market change beginning at approximately day 120 by adding large uncertainty to λ.
The predictive performance in Table 5.2 shows that the corrected models are more accurate than the standard model.

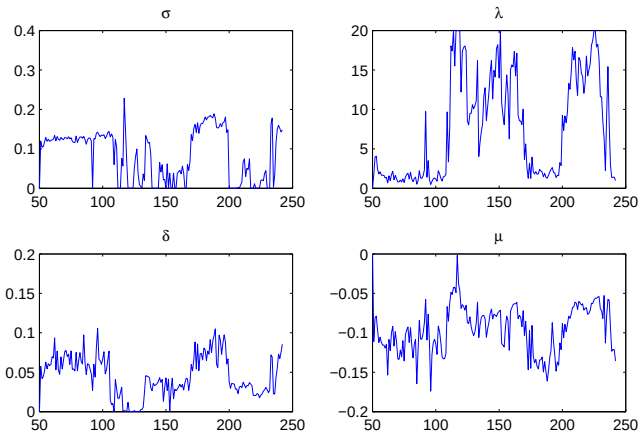

Figure 5.4: **(Merton)** Model parameters estimated in sample.

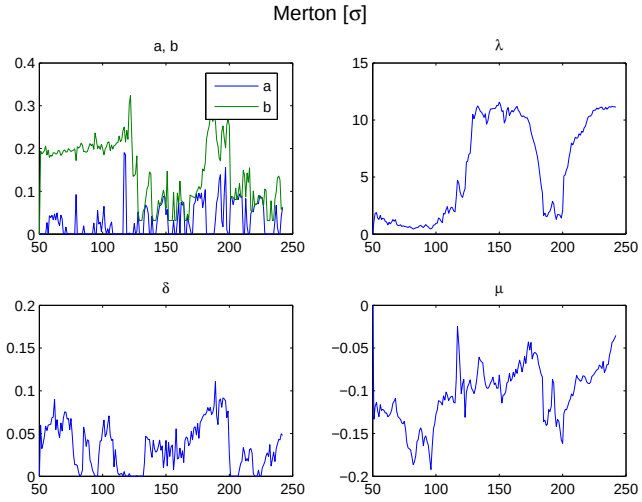

Figure 5.5: **(Merton** $[\sigma]$**)** Model parameters estimated in sample.

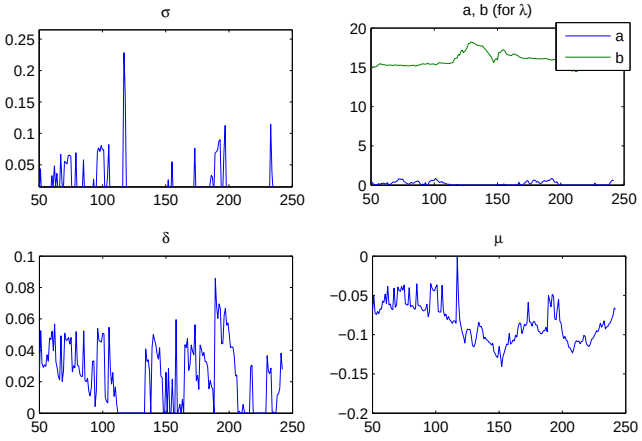

Figure 5.6: **(Merton** $[\lambda]$**)** Model parameters estimated in sample.

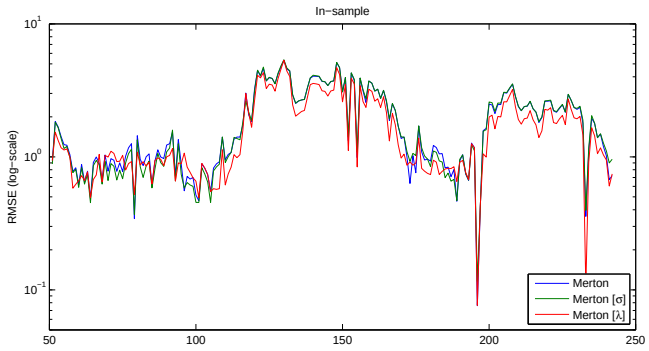

Figure 5.7: RMSE (in sample).

In sample

Model	Mean RMSE	Median RMSE
Merton	1.9109	1.4152
Merton $[\sigma]$	1.9043	1.4097
Merton $[\lambda]$	1.6680	1.1391

Out of sample

Model	Mean RMSE	Median RMSE
Merton	2.4305	2.2103
Merton $[\sigma]$	2.4138	2.0964
Merton $[\lambda]$	2.2085	1.9061

Table 5.2: Mean and median of RMSE for in-sample fit and predictions out of sample (day 50 to 246).

Heston

Estimated parameters in the Heston model is shown in Figure 5.8. The results with uncertainty in initial variance v_0 and long term Θ are illustrated in Figure 5.9 and Figure 5.10, respectively. We note that the level of uncertainty in Heston is smaller than in the BS and Merton models, suggesting that the standard Heston model may be good enough to capture the dynamics in the data set. Secondly, similar to what we could depict in the Merton models, the market seems to change starting from day 120 and the corrected models are capturing this by adding larger uncertainty. Even here, in-sample RMSE has a lower value for the modified models, although its improvement is much less evident than for the Black-Scholes and Merton models.

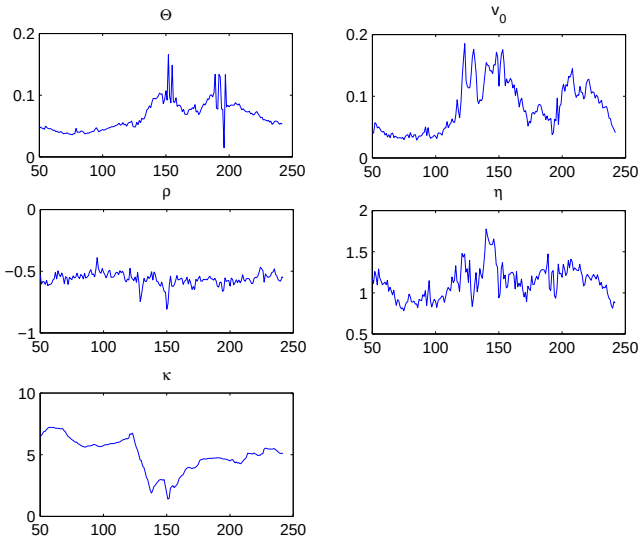

Figure 5.8: **(Heston)** Model parameters estimated in sample.

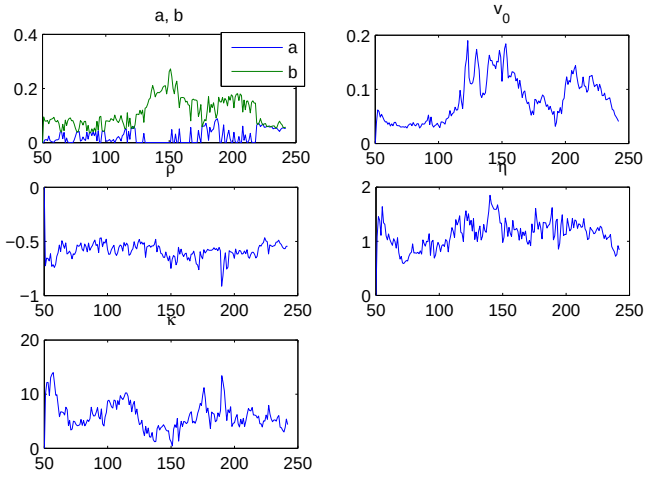

Figure 5.9: **(Heston** [Θ]**)** Model parameters estimated in sample.

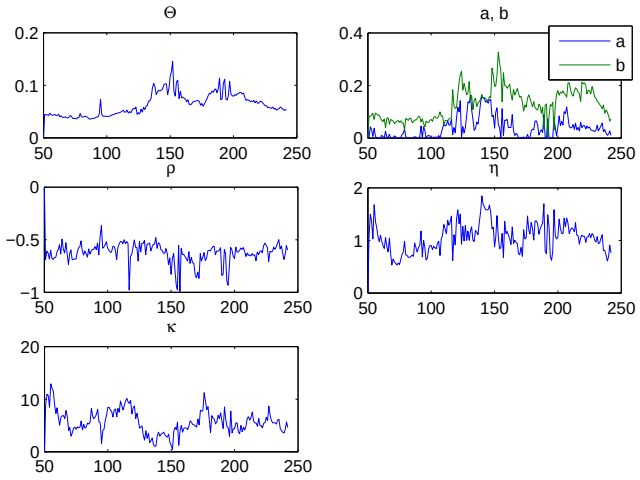

Figure 5.10: **(Heston** $[v_0]$**)** Model parameters estimated in sample.

In sample

Model	Mean RMSE	Median RMSE
Heston	0.3519	0.2853
Heston [Θ]	0.3360	0.2729
Heston [v_0]	0.3388	0.2733

Out of sample

Model	Mean RMSE	Median RMSE
Heston	1.4058	1.0318
Heston [Θ]	1.3975	1.0193
Heston [v_0]	1.4022	1.0059

Table 5.3: Mean and median of RMSE for in-sample fit and predictions out of sample (day 50 to 246).

Bates

Estimated parameters in the Bates model is shown in Figure 5.11. Results with uncertainty in the initial variance v_0, long term Θ and jump intensity λ are shown in Figures 5.12, 5.13 and 5.14, respectively. The Bates estimates look more stable than in the Merton and Heston models, although a shift in parameters can be depicted at approximately day 150. Furthermore, a minor correction seems to be acquired for the first 100 days. In fact, only a correction in λ seem to yield better estimates. This is also seen in Table 5.4. Since a more complex model (i.e. more parameters) typically gives rise to better results in sample, we would expect the corrected Bates models to yield lower RMSE than the uncorrected Bates model. Since this is not the case for corrections in Θ and v_0, we believe there may be difficulties with the convergence. We also make note that the Bates model can suffer from unstable estimates, see [13], due to the large number of model parameters.

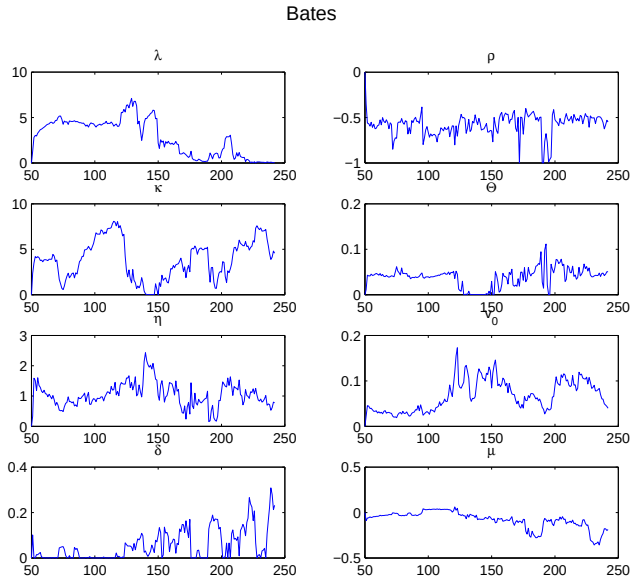

Figure 5.11: **(Bates)** Model parameters estimated in sample.

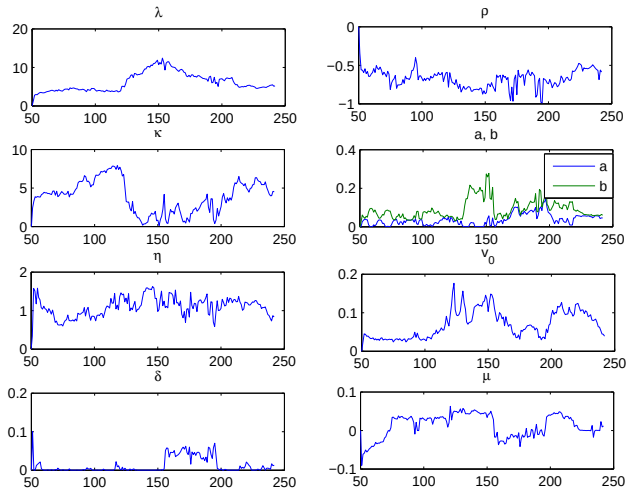

Figure 5.12: **(Bates** [Θ]**)** Parameters estimated in sample.

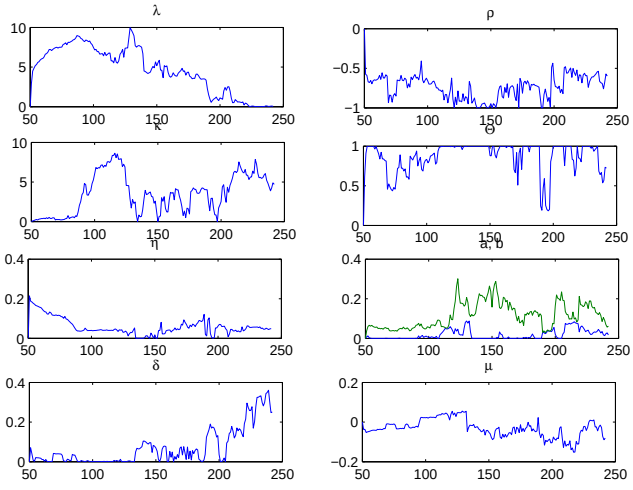

Figure 5.13: **(Bates** [v_0]**)** Parameters estimated in sample.

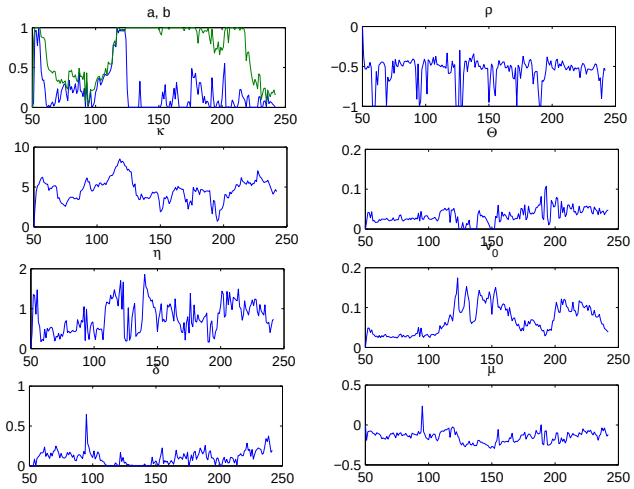

Figure 5.14: **(Bates** [λ]**)** In-sample estimation of model parameters.

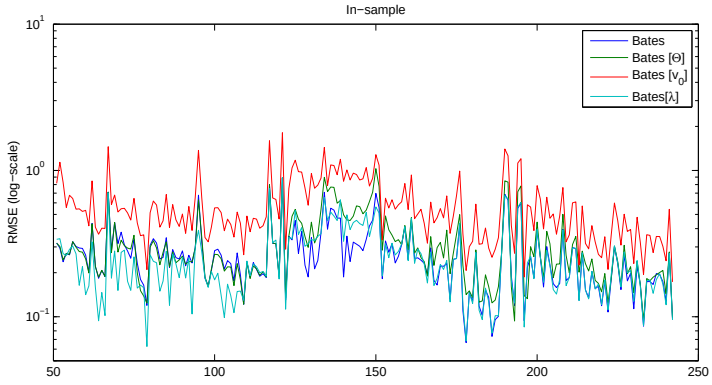

Figure 5.15: RMSE (in sample).

In sample

Model	Mean RMSE	Median RMSE
Bates	0.2690	0.2429
Bates $[\Theta]$	0.3146	0.2672
Bates $[v_0]$	0.2915	0.2565
Bates $[\lambda]$	0.2580	0.2297

Out of sample

Model	Mean RMSE	Median RMSE
Bates	1.3512	0.9962
Bates $[\Theta]$	1.4100	1.0170
Bates $[v_0]$	1.3565	1.0012
Bates $[\lambda]$	1.3497	0.9881

Table 5.4: Mean and median of RMSE for in-sample fit and predictions (day 50 to 246).

Out of sample		
Model	Mean RMSE	Median RMSE
BS	3.5653	3.2406
BS [σ]	3.4301	3.0771
Merton	2.4305	2.2103
Merton [σ]	2.4138	2.0964
Merton [λ]	2.2085	1.9061
Heston	1.4058	1.0318
Heston [Θ]	1.3975	1.0193
Heston [v_0]	1.4022	1.0059
Bates	1.3512	0.9962
Bates [Θ]	1.4100	1.0170
Bates [v_0]	1.3565	1.0012
Bates [λ]	1.3497	0.9881

Table 5.5: Summary of the mean and median of RMSE, measuring predictive performance (day 50 to 246).

Summary

Adding uncertainty to the volatility in the Bates and Merton models, and to the jump intensity in the Merton model, was found to generate lower RMSE values than their standard counterparts. In the Merton model, both standard and corrected models were found to suffer instability in a large part of the data set. The corrected Heston models seemed able to capture some of the change in market data by adding uncertainty. A minor difference in forecasting performance was found between the standard and corrected Heston models. An even smaller difference was found in the Bates model. Bates in however likely to generate unstable estimates due to the large number of parameters. Although a correction in parameter uncertainty improves the B&S and Merton models, they do not outperform the Heston and Bates models, see Table 5.5. However, adding uncertainty in the Heston model seems to improve predicitive performance to the level of the standard Bates model.

5.2 Unscented Kalman Filter

Although LS methods are known for giving the best fit in sample, the Extended Kalman filter (EKF) has become a common technique for nonlinear estimation. The filter operates recursively and is a clear improvement from a computation-time point of view. In addition, the filter was found to perform better out of sample in [13]. The basic framework for the EKF involves estimation of the state of a nonlinear dynamic system, in our case looking like

$$\theta_{t+1} = \theta_t + n_t^1 \tag{5.2.1}$$

$$y_t = f(\theta_t) + n_t^2, \tag{5.2.2}$$

where θ_t represents the unobserved parameter state of the system and y_t is the observed signal. The noise process n^1 drives the system and n^2 is the measurement noise for the observations, see [16]. The measurement function f will be the pricing formula for each method. The EKF is a heavily used for recursive maximum-likelihood estimation of the state θ_t. As discussed in [10], the EKF can have poor performance for a highly nonlinear function f which is why this thesis uses the unscented kalman filter (UKF). The idea is to produce several sampling points (using a sampling technique called the unscented transform) around the current state estimate based on its covariance. Propagating these points (called sigma points) through the nonlinear map will then result in more accurate estimation of the mean and covariance. The Matlab-function 'ukf' was used for the implementation. For each model, the parameters were estimated for the first 100 trading days using different state and measurement covariance matrices. The variance giving the lowest RMSE was chosen to re-fit the model. In general, volatilities were assigned variances of size 0.0001 to 0.001, and jump intensities of size 0.001 to 0.1. There is a reason to why we start the estimation at day 50 and not day 100. The data set seems to differ in behaviour depending on whether we are looking before or after day 120. We therefore begin at day 50, attempting to capture the performance in both parts.

5.2.1 Results

Black&Scholes

The result for the B&S models are similar to the ones using LS with penalty in the previous section. The filter gives rise to smoother estimates, but RMSE in general is larger than when using the LS method.

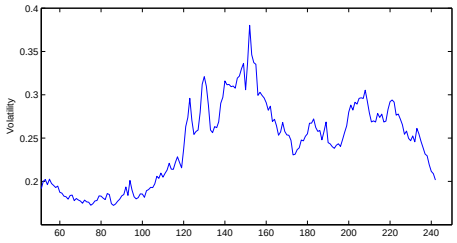

Figure 5.16: **(Black-Scholes)** Estimated volatility in sample.

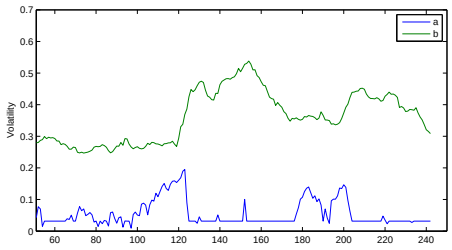

Figure 5.17: **(Black-Scholes** $[\sigma]$**)** Parameters a and b estimated in sample, where $\sigma \in U(a, b)$.

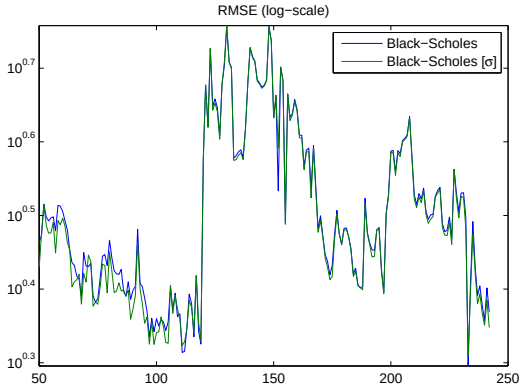

Figure 5.18: RMSE (in sample).

In-sample

Model	Mean RMSE	Median RMSE
BS	3.2594	3.0364
BS $[\sigma]$	3.2199	2.9968

Out-of-sample

Model	Mean RMSE	Median RMSE
BS	3.5626	3.2286
BS $[\sigma]$	3.5186	3.1446

Table 5.6: Mean and median of RMSE for in-sample fit and predictions out of sample (day 50 to 246).

Merton

We recall the difficulties in previous section, where the Merton models with LS-estimates suffered from instability. With the UKF, the λ-parameter is given more realistic values in Figure 5.20 and Figure 5.20. A shift in the parameters is still occurring around the 120-th day. From Table 5.7 we see that the forecasting performance has been significantly improved for the model with a correction in the jump intensity, compared to the results using the LS-estimate.

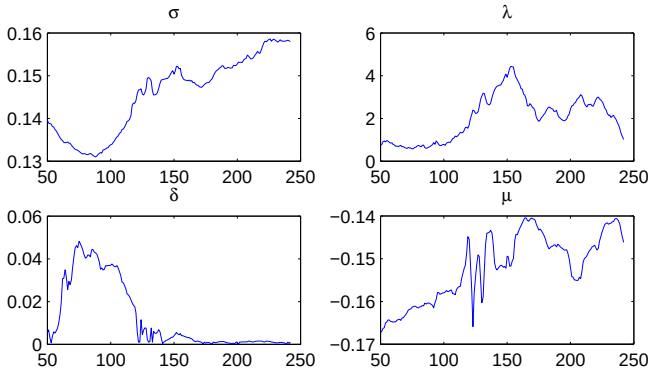

Figure 5.19: **(Merton)** Parameters estimated in sample.

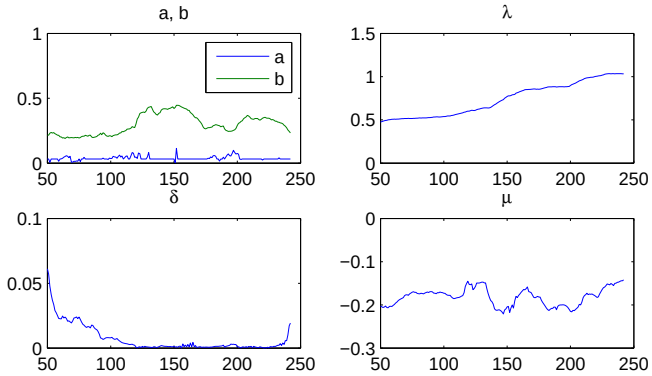

Figure 5.20: **(Merton** $[\sigma]$**)** Parameters estimated in sample.

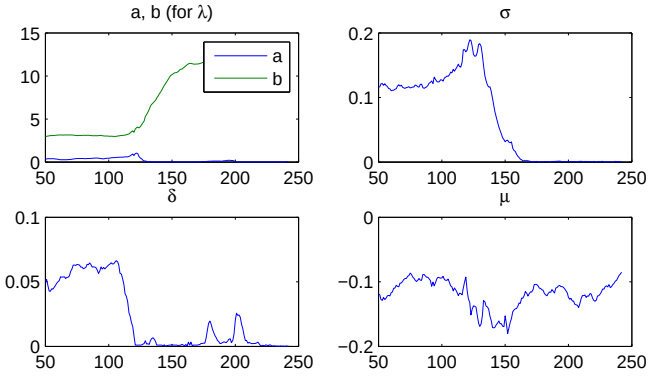

Figure 5.21: **(Merton** [λ]**)** Parameters estimated in sample.

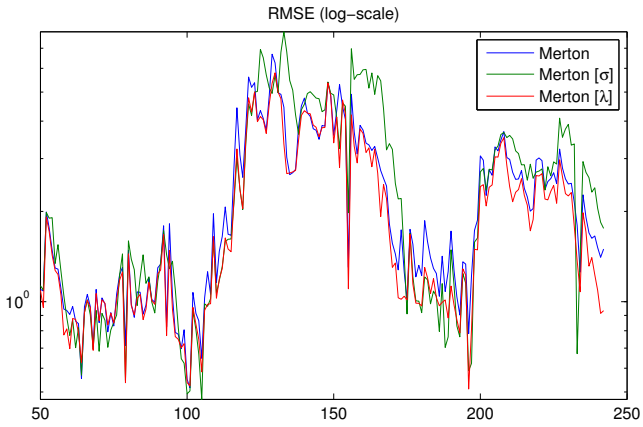

Figure 5.22: RMSE (in sample)

In sample

Model	Mean RMSE	Median RMSE
Merton	2.2338	1.7609
Merton $[\sigma]$	2.5552	1.9826
Merton $[\lambda]$	1.8520	1.4098

Out of sample

Model	Mean RMSE	Median RMSE
Merton	2.6401	2.2777
Merton $[\sigma]$	2.9540	2.5555
Merton $[\lambda]$	2.3284	1.8867

Table 5.7: Mean and median of RMSE for in-sample fit and out-of-sample predictions (day 50 to 246).

Heston

The Heston models with UKF seems to be more sensitive to the market change then the corresponding models with penalized LS. Performance in predictions is worse than with the LS method.

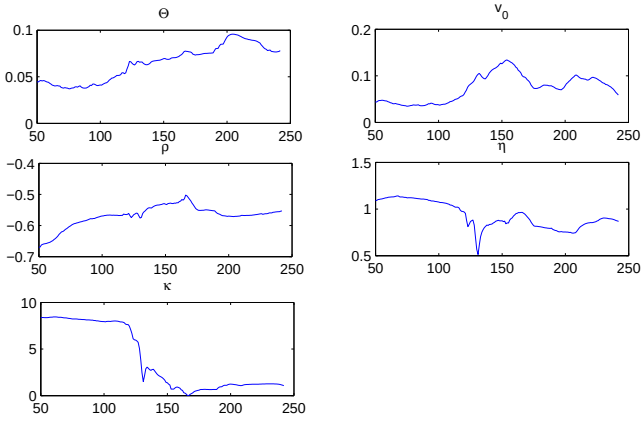

Figure 5.23: **(Heston)** Parameters estimated in sample.

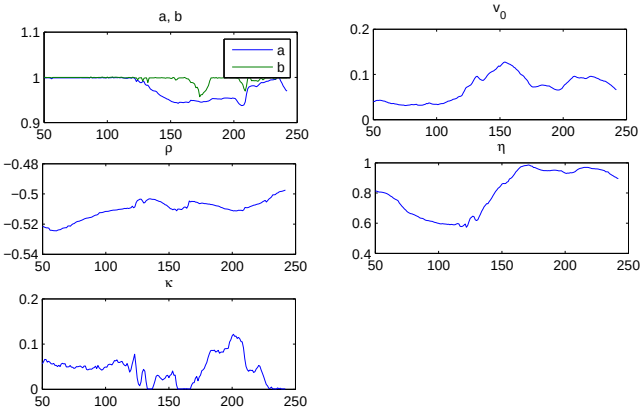

Figure 5.24: **(Heston** [Θ]**)** Parameters estimated in sample.

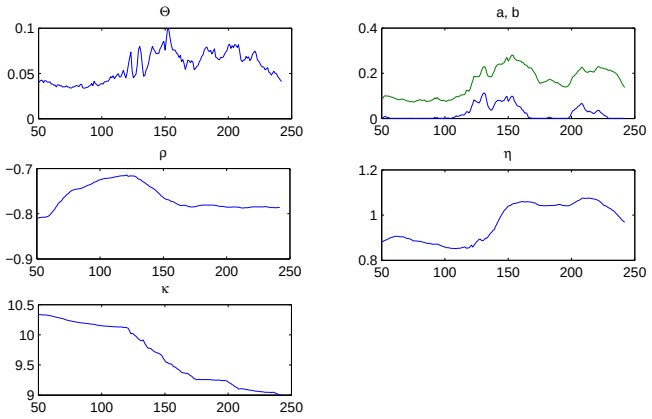

Figure 5.25: **(Heston** $[v_0]$**)** Parameters estimated in sample.

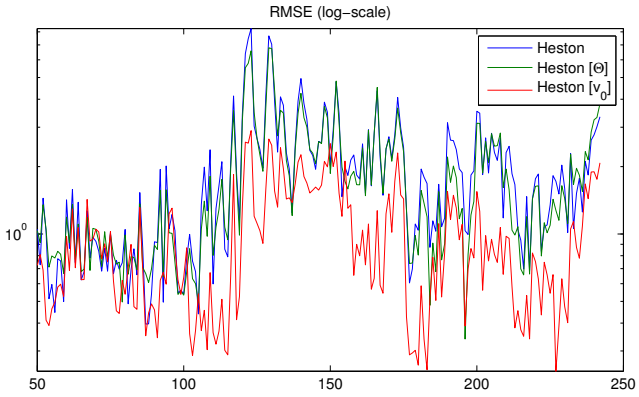

Figure 5.26: RMSE (in sample)

In sample

Model	Mean RMSE	Median RMSE
Heston	1.9011	1.6631
Heston $[\sigma]$	1.7691	1.4294
Heston $[v_0]$	0.9773	0.7862

Out of sample

Model	Mean RMSE	Median RMSE
Heston	2.3047	2.0374
Heston $[\sigma]$	2.2142	1.9041
Heston $[v_0]$	1.6465	1.3686

Table 5.8: Mean and median of RMSE for in-sample fit and out-of-sample predictions (day 50 to 246).

Bates

Difficulties in estimating the Bates model arose when the LS method was used. The similar can be found when using the UKF.

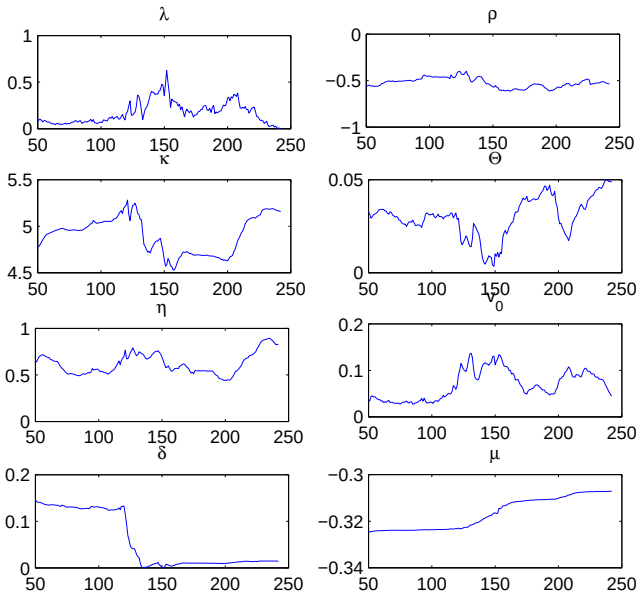

Figure 5.27: **(Bates)** In-sample estimation of model parameters.

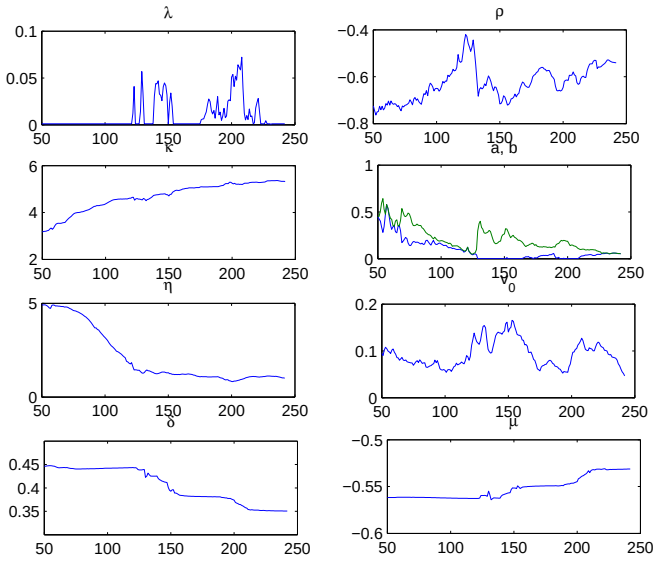

Figure 5.28: **(Bates** [Θ]**)** In-sample estimation of model parameters.

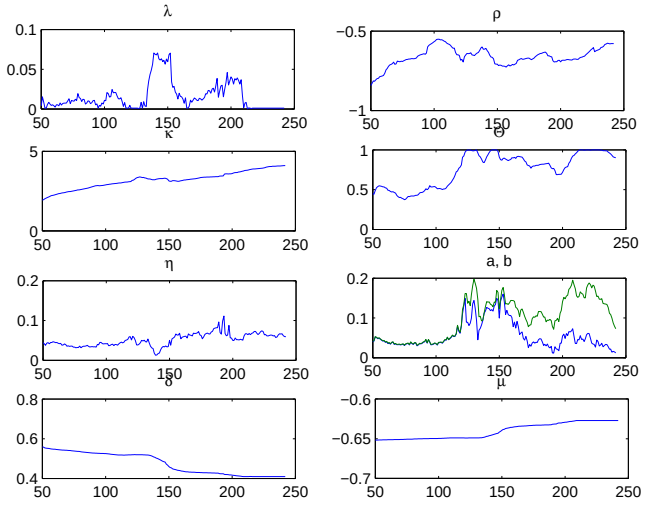

Figure 5.29: **(Bates** [v_0]**)** In-sample estimation of model parameters.

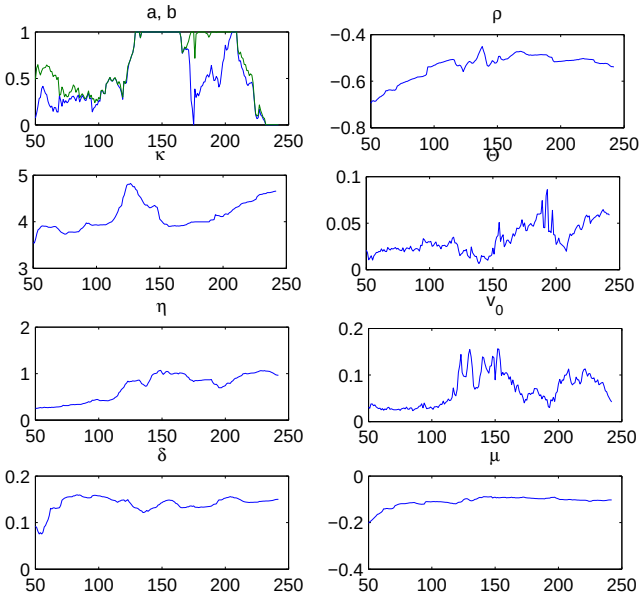

Figure 5.30: **(Bates** [λ]**)** In-sample estimation of model parameters.

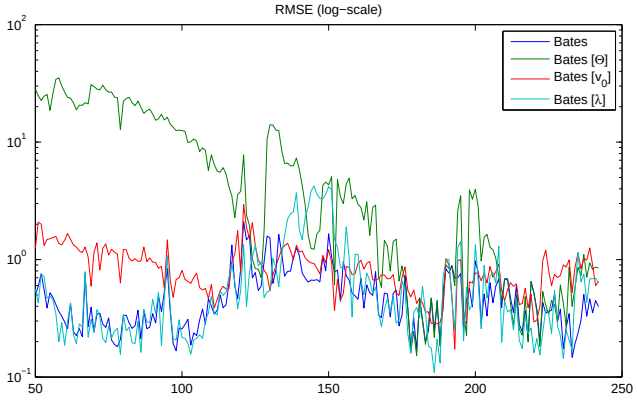

Figure 5.31

In sample

Model	Mean RMSE	Median RMSE
Bates	0.5191	0.4259
Bates $[\Theta]$	7.9783	3.2938
Bates $[v_0]$	0.8753	0.8295
Bates $[\lambda]$	0.7093	0.4232

Out of sample

Model	Mean RMSE	Median RMSE
Bates	1.3998	1.0204
Bates $[\Theta]$	8.3500	4.0071
Bates $[v_0]$	1.6294	1.2243
Bates $[\lambda]$	1.5714	1.1397

Table 5.9: Mean and median of RMSE for in-sample fit and out-of-sample predictions (day 50 to 246).

	UKF		LS	
Model	Mean RMSE	Median RMSE	Mean RMSE	Median RMSE
BS	3.5626	3.2286	3.5653	3.2406
BS $[\sigma]$	3.5186	3.1446	3.4301	3.0771
Merton	2.6401	2.2777	2.4305	2.2103
Merton $[\sigma]$	2.9540	2.5555	2.4138	2.0964
Merton $[\lambda]$	2.3284	1.8867	2.2085	1.9061
Heston	2.3047	2.0374	1.4058	1.0318
Heston $[\sigma]$	2.2142	1.9041	1.3975	1.0193
Heston $[v_0]$	1.6465	1.3686	1.4022	1.0059
Bates	1.3998	1.0204	1.3512	0.9962
Bates $[\Theta]$	8.3500	4.0071	1.4100	1.0170
Bates $[v_0]$	1.6294	1.2243	1.3565	1.0012
Bates $[\lambda]$	1.5714	1.1397	1.3497	0.9881

Table 5.10: Summary of the mean and median of RMSE, measuring predictive performance for day 50 to 246.

Summary

Using the UKF resulted in smoother estimates and an overall deterioration for in-sample as well as out-of-sample performance. However, one clear improvement (based on RMSE) was found with the Merton model with correction in λ. One could try to improve the filter further by transforming the states, e.g. using $\theta = \ln(\theta)$. This will prevent undesired estimates such as negative volatilities. Moreover, greater effort can be made to find better covariance matrices for the filter. Seeing as the UKF has a clear advantage in computational time, an attempt to improve it would probably be worth while. A summary of predictive performance can be found in Table 5.10. The corrected models will in general out-perform the standard models. This is particularly noticeable for the B&S and Merton models. A less significant improvement was found in Heston. The Bates model was not found to be improved by a correction in the parameter uncertainty. However, it is not unusual to receive unstable estimates since there is a large number of parameters in the Bates model. Still, the Bates model is typically better at modeling stock prices. The clear winners are the Heston and Bates models estimated with the penalized LS method. We note that adding uncertainty into the standard Heston model will improve the prediction performance, lowering RMSE to the level of the Bates model. This suggests that the corrected Heston model is to prefer since it has fewer parameters than the Bates model.

Chapter 6

CONCLUSIONS

This thesis has shown that a correction in parameter uncertainty can be computed for some parameters for a large variety of models within the Fourier framework. Our only requirement is of the characteristic function to be well-defined and exponentially affine in the parameter of interest.
Adding uncertainty to different types of volatilities (volatility, initial volatility and long term volatility) was found to generate a volatility smile in a simulation study. The result is beneficial since it is consistent with empirical observations. A corrections in the jump intensity was found to generate minor gains, suggesting that the Merton and Bates models are robust against misspecifiation of the jump intensity. However, since the empirical study showed that a correction in the jump intensity would improve the Merton and Bates models, this suggests that we should have allowed the jump intensity to vary more in the uniform distribution, i.e. we should have considered a wider interval (a, b) in the uniform distribution.
The empirical study showed that a correction in the Black&Scholes and Merton models improves the performance in sample and out of sample significantly. A correction in the initial volatility in the Heston model was found to improve the performance to the level of the standard Bates model. The corrected Heston model is therefore preferrable since it has fewer parameters. The Bates model was not found to benefit from a correction in the investigated parameters, suggesting that any gain generated by a correction may be over-shadowed by the drawbacks of adding parameters to the model.

6.1 Further work

Generalizing the uncertainty to several parameters at the same time should be an easy task. The main concern may lie in obtaining a suitable multivariate distribution function. If we can assume the parameters to be independent of each other, the joint distribution would simply be the product of marginal distributions. Seeing as it is a rather unrealistic assumption, one could try to use the theory of Copulas.
Furthermore, it would be interesting to apply the method derived in this thesis to Lévy-processes. For example, the Normal Inverse Gaussian process seems to have a characteristic function which is exponentially affine in at least one parameter.

Appendix A

TRIANGULAR DISTRIBUTION IN THE B&S MODEL

Uncertainty was added in the volaility σ^2 in the B&S model, see Section 4.2. The result where σ^2 is assumed to follow a triangular distribution is shown in Figure A.1. We see that the result is similar to the findings in Section 4.2 and that the shape of the uncertainty seems to be of minor importance. The variance of the uncertainty, rather than the specific distribution seems to matter. This is consistent with some of the findings in non-parametric regression, arguing that it is the bandwidth and not the type of kernel that is of most importance.

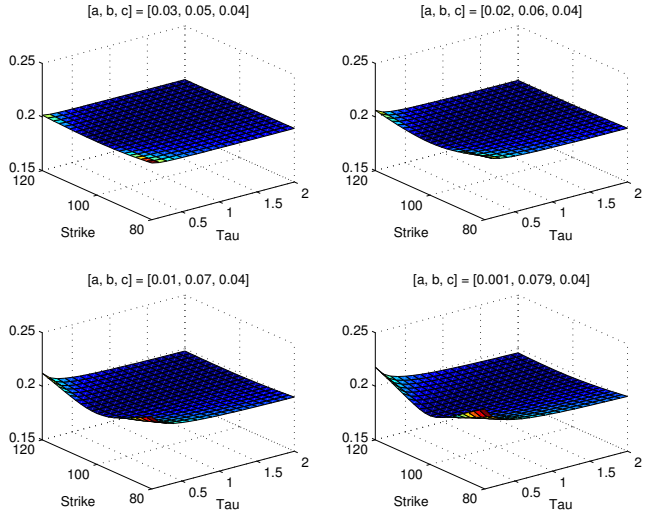

Figure A.1: **(Black-Scholes)** Implied volatility in the corrected model for increasing level of parameter uncertainty, i.e. wider interval $[a, b]$ in the triangular distribution using $c = 0.04$.

BIBLIOGRAPHY

[1] Sebastian Åberg, *Derivative pricing, lecture notes to fms170/masm19*, Lund University, 2010.

[2] Sara Biagini and Rama Cont, *Model-free representation of pricing rules as conditional expectations*, Stochastic processes and applications to mathematical finance (2006), 53–66.

[3] Thomas Björk, *Arbitrage theory in continuous time*, Oxford University Press Inc., New York, 2009.

[4] R.L. Burden and Faires J.D., *Numerical analysis*, ninth ed., Brooks/Cole, 2010.

[5] Peter Carr and Dilip Madan, *Option valuation using the fast fourier transform*, Journal of computational finance **2** (1999), no. 4, 61–73.

[6] Rama Cont and Peter Tankov, *Financial modelling with jump processes*, Chapman & Hall/CRC: London, 2004.

[7] Sebastien del Bano Rollin and Alberto Ferreiro-Castilla, *A new look at the heston characteristic function*, pre-print (2009).

[8] Allan Gut, *An intermediate course in probability*, second ed., Springer Texts in Statistics, Springer, New York, 2009. MR 2528081 (2010k:60001)

[9] Ali Hirsa, *Computational methods in finance*, CRC Press, 2012.

[10] Simon J. Julier and Jeffrey K. Uhlmann, *A new extension of the kalman filter to nonlinear systems*, 1997, pp. 182–193.

[11] Erik Lindström, *Implications of parameter uncertainty on option prices*, Advances in Decision Sciences **2010** (2010).

[12] Erik Lindström and Johan Strålfors, *Model uncertainty, model selection and option valuation*, 34. Symposium i Anvendt Statistik, Danmarks Statistik & Copenhagen Business School, 2012, pp. 229–238.

[13] Erik Lindström, Jonas Ströjby, Mats Brodén, Magnus Wiktorsson, and Jan Holst, *Sequential calibration of options*, Computational Statistics & Data Analysis **52** (2008), no. 6, 2877–2891.

[14] A. N. Shiryaev, *Probability*, second ed., Graduate Texts in Mathematics, vol. 95, Springer-Verlag, New York, 1996, Translated from the first (1980) Russian edition by R. P. Boas. MR 1368405 (97c:60003)

[15] Elias M. Stein and Rami Shakarchi, *Fourier analysis*, Princeton Lectures in

Analysis, vol. 1, Princeton University Press, Princeton, NJ, 2003, An introduction. MR 1970295 (2004a:42001)

[16] E.A. Wan and R Van der Merwe, *The unscented kalman filter for nonlinear estimation*, Adaptive Systems for Signal Processing, Communications, and Control Symposium (2000).